

# Approximation of the Boltzmann Collision Operator Based on Hermite Spectral Method

Yanli Wang\*, Zhenning Cai†

June 18, 2019

## Abstract

Based on the Hermite expansion of the distribution function, we introduce a Galerkin spectral method for the spatially homogeneous Boltzmann equation with the realistic inverse-power-law models. A practical algorithm is proposed to evaluate the coefficients in the spectral method with high accuracy, and these coefficients are also used to construct new computationally affordable collision models. Numerical experiments show that our method captures the low-order moments very efficiently.

**Keywords:** Boltzmann equation, Hermite spectral method, inverse power law

## 1 Introduction

Over a century ago, Boltzmann devised a profound equation describing the statistical behavior of gas molecules. A number of interesting theoretical and practical problems emerged due to the birth of this equation, among which the numerical simulation for this six-dimensional Boltzmann equation is one significant topic after the invention of computers. The difficulty comes partly from its high dimensionality, and partly from its complicated integral operator modeling the binary collision of gas molecules. People have been using the Monte Carlo method [3] to overcome the difficulty caused by high dimensionality, but nowadays, a six-dimensional simulation using a deterministic solver is no longer unaffordable due to the fast growth of computer flops. Fully six-dimensional computations are carried out in [25, 11] for the simplified BGK-type collision terms. However, numerical simulation of the original Boltzmann equation with the binary collision operator still requires a large amount of computational resources [12].

Currently, the deterministic discretization of the binary collision operator can be categorized into three types: the discrete velocity method [20, 33], the Fourier spectral method [34, 16], and the Hermite spectral method [22, 17]. The discrete velocity method is hardly used in the numerical simulation due to its low order of convergence [33], whereas the Fourier spectral method is more popular because of its fast convergence rate and high numerical efficiency. For hard-sphere gases, the computational cost can be reduced to  $O(KN \log N)$  [32, 14], with  $K$  being the number of discrete points on the unit sphere and  $N$  being the total number of modes in the velocity space. For general gas molecules, the Fourier spectral method has time complexity  $O(N^2)$  [34] or  $O(KN^{4/3} \log N)$  [16]. Based on these works, some improved versions of the Fourier spectral methods have been proposed [18, 35, 15, 4], and some spatially inhomogeneous

\*Department of Engineering, Peking University, Beijing, China, 100871, email: wang\_yanli@pku.edu.cn.

†Department of Mathematics, National University of Singapore, Level 4, Block S17, 10 Lower Kent Ridge Road, Singapore 119076, email: matcz@nus.edu.sg.

applications have been carried out [40, 12]. We would also like to refer the readers to the review article [13] for a complete review of the above methods.

Compared with the Fourier spectral method which requires periodization of the distribution function, the Hermite spectral method looks more natural since the basis functions with orthogonality in  $\mathbb{R}^3$  are employed. In fact, the Hermite spectral method has a longer history and has been known as the moment method since Grad's work [21]. Grad proposed in [21] a general method to find the expansion of the binary collision term with Hermite basis functions. Later, a similar way to expand the binary collision term using Sonine polynomials (also known as spherical Hermite polynomials) was proposed in [31]. The techniques used in formulating the expansion are also introduced in the book [39].

Despite these works, the Hermite spectral method is used in the numerical simulation only until recently [22, 17, 30]. There are two major difficulties in applying this method: one is the evaluation of the coefficients in the expansion of the collision operator; the other is the huge computational cost due to its quadratic form. Although the general procedure to obtain the coefficients is given in [21, 39], following such a procedure involves expansion of a large number of huge polynomials, which is quite expensive even for a modern computer algebraic system; Kumar [31] provided a formula in his expansion using Sonine polynomials, while the formula involves evaluation of a large number of Talmi coefficients, which is not tractable either. As for the computational cost, the computational time of one evaluation of the collision operator is proportional to the cube of the number of degrees of freedom, while in the Fourier spectral method, the time complexity for a direct Galerkin discretization is only the square of the number of modes.

This work is devoted to both of the aforementioned issues. On one hand, by using a number of properties for relevant polynomials, we provide explicit formulas for all the coefficients appearing in the expansion of the collision operator with the Hermite spectral method. These formulas are immediately applicable in the sense of coding, and the computational cost is affordable for a moderate number of degrees of freedom. On the other hand, we combine the modeling strategy and the numerical technique to form a new way to discretize the collision term, where only a portion in the truncated series expansion is treated "quadratically", and the remaining part just decays exponentially as in the BGK model. Thus the computational cost is greatly reduced and we can still capture the evolution of low-order moments accurately.

The rest of this paper is organized as follows. In Section 2, we briefly review the Boltzmann equation and the Hermite expansion of the distribution function. In Section 3, we first give an explicit expression for the series expansion of the quadratic collision operator, and then construct approximate collision models based on such an expansion. Some numerical experiments verifying our method are carried out in Section 4. Some concluding remarks, as well as some comparison with similar works, are made in Section 5. Detailed derivation of the expansion is given in the Appendix.

## 2 Boltzmann equation and Hermite expansion of the distribution function

This section is devoted to the introduction of existing works needed by our further derivation. We will first give a brief review of the Boltzmann equation and the IPL (Inverse-Power-Law) model, and then introduce the expansion of the distribution function used in the Hermite spectral method.

## 2.1 Boltzmann equation

The Boltzmann equation describes the fluid state using a distribution function  $f(t, \mathbf{x}, \mathbf{v})$ , where  $t$  is the time,  $\mathbf{x}$  is the spatial coordinates, and  $\mathbf{v}$  stands for the velocity of gas molecules. The governing equation of  $f$  is

$$\frac{\partial f}{\partial t} + \nabla_{\mathbf{x}} \cdot (\mathbf{v}f) = \mathcal{Q}[f], \quad t \in \mathbb{R}^+, \quad \mathbf{x} \in \mathbb{R}^3, \quad \mathbf{v} \in \mathbb{R}^3, \quad (2.1)$$

where  $\mathcal{Q}[f]$  is the collision operator which has a quadratic form

$$\mathcal{Q}[f](t, \mathbf{x}, \mathbf{v}) = \int_{\mathbb{R}^3} \int_{\mathbf{n} \perp \mathbf{g}} \int_0^\pi [f(t, \mathbf{x}, \mathbf{v}')f(t, \mathbf{x}, \mathbf{v}') - f(t, \mathbf{x}, \mathbf{v}_1)f(t, \mathbf{x}, \mathbf{v})] B(|\mathbf{g}|, \chi) d\chi d\mathbf{n} d\mathbf{v}_1, \quad (2.2)$$

where  $\mathbf{g} = \mathbf{v} - \mathbf{v}_1$  and  $\mathbf{n}$  is a unit vector. Hence  $\int_{\mathbf{n} \perp \mathbf{g}} \cdots d\mathbf{n}$  is a one-dimensional integration over the unit circle perpendicular to  $\mathbf{g}$ . The post-collisional velocities  $\mathbf{v}'$  and  $\mathbf{v}'_1$  are

$$\begin{aligned} \mathbf{v}' &= \cos^2(\chi/2)\mathbf{v} + \sin^2(\chi/2)\mathbf{v}_1 - |\mathbf{g}| \cos(\chi/2) \sin(\chi/2)\mathbf{n}, \\ \mathbf{v}'_1 &= \cos^2(\chi/2)\mathbf{v}_1 + \sin^2(\chi/2)\mathbf{v} + |\mathbf{g}| \cos(\chi/2) \sin(\chi/2)\mathbf{n}, \end{aligned} \quad (2.3)$$

and from the conservation of momentum and energy, it holds that

$$\mathbf{v} + \mathbf{v}_1 = \mathbf{v}' + \mathbf{v}'_1, \quad |\mathbf{v}|^2 + |\mathbf{v}_1|^2 = |\mathbf{v}'|^2 + |\mathbf{v}'_1|^2. \quad (2.4)$$

The collision kernel  $B(|\mathbf{g}|, \chi)$  is a non-negative function determined by the force between gas molecules.

In this paper, we are mainly concerned with the IPL model, for which the force between two molecules is always repulsive and proportional to a negative power of their distance. In this case, the kernel  $B(|\mathbf{g}|, \chi)$  in (2.2) has the form

$$B(|\mathbf{g}|, \chi) := |\mathbf{g}|^{\frac{\eta-5}{\eta-1}} W_0 \left| \frac{dW_0}{d\chi} \right|, \quad \eta > 3, \quad (2.5)$$

where  $-\eta$  is the index in the power of distance. The case  $\eta > 5$  corresponds to the ‘‘hard potential’’, and the case  $3 < \eta < 5$  corresponds to the ‘‘soft potential’’. When  $\eta = 5$ , the collision kernel  $B(|\mathbf{g}|, \chi)$  is independent of  $|\mathbf{g}|$ , and in this model the gas molecules are called ‘‘Maxwell molecules’’. The dimensionless impact parameter  $W_0$  is related to the angle  $\chi$  by

$$\chi = \pi - 2 \int_0^{W_1} \left[ 1 - W^2 - \frac{2}{\eta-1} \left( \frac{W}{W_0} \right)^{\eta-1} \right]^{-1/2} dW, \quad (2.6)$$

and  $W_1$  is a positive real number satisfying

$$1 - W_1^2 - \frac{2}{\eta-1} \left( \frac{W_1}{W_0} \right)^{\eta-1} = 0. \quad (2.7)$$

It can be easily shown that the above equation of  $W_1$  admits a unique positive solution when  $\eta > 3$  and  $W_0 > 0$ .

Apparently, the quadratic collision term is the most complicated part in the Boltzmann equation. In this paper, we will focus on the numerical approximation of  $\mathcal{Q}[f]$ . For simplicity,

we assume that the gas is homogeneous in space, and thus we can remove the variable  $\mathbf{x}$  in the distribution function to get the spatially homogeneous Boltzmann equation

$$\frac{\partial f}{\partial t} = \mathcal{Q}[f], \quad t \in \mathbb{R}^+, \quad \mathbf{v} \in \mathbb{R}^3. \quad (2.8)$$

It is well known that the steady state of this equation takes the form of the Maxwellian:

$$f(\infty, \mathbf{v}) = \mathcal{M}_{\rho, \mathbf{u}, \theta}(\mathbf{v}) := \frac{\rho}{(2\pi\theta)^{3/2}} \exp\left(-\frac{|\mathbf{v} - \mathbf{u}|^2}{2\theta}\right), \quad (2.9)$$

where the density  $\rho$ , velocity  $\mathbf{u}$  and temperature  $\theta$  can be obtained by

$$\rho = \int_{\mathbb{R}^3} f(t, \mathbf{v}) d\mathbf{v}, \quad \mathbf{u} = \frac{1}{\rho} \int_{\mathbb{R}^3} \mathbf{v} f(t, \mathbf{v}) d\mathbf{v}, \quad \theta = \frac{1}{3\rho} \int_{\mathbb{R}^3} |\mathbf{v} - \mathbf{u}|^2 f(t, \mathbf{v}) d\mathbf{v}. \quad (2.10)$$

These quantities are invariant during the evolution, and therefore (2.10) holds for any  $t$ . By selecting proper frame of reference and applying appropriate non-dimensionalization, we can obtain

$$\rho = 1, \quad \mathbf{u} = 0, \quad \theta = 1, \quad (2.11)$$

and thus the Maxwellian (2.9) is reduced to

$$\mathcal{M}(\mathbf{v}) := \frac{1}{(2\pi)^{3/2}} \exp\left(-\frac{|\mathbf{v}|^2}{2}\right). \quad (2.12)$$

Hereafter, the normalization (2.11) will always be assumed.

In the literature, people have been trying to avoid the complicated form of the collision operator  $\mathcal{Q}[f]$  by introducing simpler approximations to it. For example, the BGK collision model

$$\mathcal{Q}^{\text{BGK}}[f] = \frac{1}{\tau}(\mathcal{M} - f) \quad (2.13)$$

was proposed in [2]. Here  $\tau$  is the mean relaxation time, which is usually obtained from the first approximation of the Chapman-Enskog theory [9]. When (2.13) is used to approximate the IPL model,

$$\tau = \frac{5}{2^{\frac{3\eta-7}{\eta-1}} \sqrt{\pi} A_2(\eta) \Gamma(4 - 2/(\eta - 1))}, \quad (2.14)$$

where  $A_2(\eta) = \int_0^{+\infty} W_0 \sin^2 \chi dW_0$ . With  $\mathcal{Q}[f]$  replaced by  $\mathcal{Q}^{\text{BGK}}[f]$  in (2.8), the collision process becomes an exponential convergence to the Maxwellian. Such a simple approximation provides incorrect Prandtl number 1. Hence some other models such as the Shakhov model [37] and ES-BGK model [23] are later proposed to fix the Prandtl number by changing the Maxwellian in (2.13) to a non-equilibrium distribution function. We will call these models ‘‘BGK-type models’’ hereafter.

Numerical evaluations on these BGK-type models can be found in [19, 10], where one can find that these approximations are not accurate enough when the non-equilibrium is strong. Hence the study on efficient numerical methods for the original Boltzmann equation with the quadratic collision operator is still necessary.



## 2.2 Series expansion of the distribution function

Our numerical discretization will be based on the following series expansion of the distribution function in the weighted  $L^2$  space  $\mathcal{F} = L^2(\mathbb{R}^3; \mathcal{M}^{-1} d\mathbf{v})$ :

$$f(t, \mathbf{v}) = \sum_{k_1 k_2 k_3} f_{k_1 k_2 k_3}(t) H^{k_1 k_2 k_3}(\mathbf{v}) \mathcal{M}(\mathbf{v}), \quad (2.15)$$

where  $\mathcal{M}(\mathbf{v})$  is the Maxwellian, and we have used the abbreviation

$$\sum_{k_1 k_2 k_3} := \sum_{k_1=0}^{+\infty} \sum_{k_2=0}^{+\infty} \sum_{k_3=0}^{+\infty}. \quad (2.16)$$

In (2.15),  $H^{k_1 k_2 k_3}(\mathbf{v})$  are the Hermite polynomials defined as follows:

**Definition 1** (Hermite polynomials). *For  $k_1, k_2, k_3 \in \mathbb{N}$ , the Hermite polynomial  $H^{k_1 k_2 k_3}(\mathbf{v})$  is defined as*

$$H^{k_1 k_2 k_3}(\mathbf{v}) = \frac{(-1)^n}{\mathcal{M}(\mathbf{v})} \frac{\partial^{k_1+k_2+k_3}}{\partial v_1^{k_1} \partial v_2^{k_2} \partial v_3^{k_3}} \mathcal{M}(\mathbf{v}), \quad (2.17)$$

where  $\mathcal{M}(\mathbf{v})$  is given in (2.12).

The expansion (2.2) was proposed by Grad in [21], where such an expansion was used to derive moment methods. The relation between the coefficients  $f_{k_1 k_2 k_3}$  and the moments can be seen from the orthogonality of Hermite polynomials

$$\int_{\mathbb{R}^3} H^{k_1 k_2 k_3}(\mathbf{v}) H^{l_1 l_2 l_3}(\mathbf{v}) \mathcal{M}(\mathbf{v}) d\mathbf{v} = \delta_{k_1 l_1} \delta_{k_2 l_2} \delta_{k_3 l_3} k_1! k_2! k_3!. \quad (2.18)$$

For example, by the above orthogonality, we can insert the expansion (2.15) into the definition of  $\rho$  in (2.10) to get  $f_{000} = \rho$ . In our case, the normalization (2.11) gives us  $f_{000} = 1$ . Similarly, it can be deduced from the other two equations in (2.10) and (2.11) that

$$f_{100} = f_{010} = f_{001} = 0, \quad f_{200} + f_{020} + f_{002} = 0. \quad (2.19)$$

Other interesting moments include the heat flux  $q_i$  and the stress tensor  $\sigma_{ij}$ , which are defined as

$$q_i = \frac{1}{2} \int_{\mathbb{R}^3} |\mathbf{v} - \mathbf{u}|^2 (v_i - u_i) f d\mathbf{v} = \frac{1}{2} \int_{\mathbb{R}^3} |\mathbf{v}|^2 v_i f d\mathbf{v}, \quad i = 1, 2, 3,$$

$$\sigma_{ij} = \int_{\mathbb{R}^3} \left( (v_i - u_i)(v_j - u_j) - \frac{1}{3} \delta_{ij} |\mathbf{v} - \mathbf{u}|^2 \right) f d\mathbf{v} = \int_{\mathbb{R}^3} \left( v_i v_j - \frac{1}{3} \delta_{ij} |\mathbf{v}|^2 \right) f d\mathbf{v}, \quad i, j = 1, 2, 3.$$

They are related to the coefficients by

$$q_1 = 3f_{300} + f_{120} + f_{102}, \quad q_2 = 3f_{030} + f_{210} + f_{012}, \quad q_3 = 3f_{003} + f_{201} + f_{021},$$

and

$$\begin{aligned} \sigma_{11} &= 2f_{200}, & \sigma_{12} &= f_{110}, & \sigma_{13} &= f_{101}, \\ \sigma_{22} &= 2f_{020}, & \sigma_{23} &= f_{011}, & \sigma_{33} &= 2f_{002}. \end{aligned}$$

### 3 Approximation of the collision term

To get the evolution of the coefficients  $f_{k_1 k_2 k_3}$  in the expansion (2.15), we need to expand the collision term using the same basis functions. The expansions of the BGK-type collision operators are usually quite straightforward. For instance, the series expansion of the BGK collision term (2.13) is given in [7] as

$$\mathcal{Q}^{\text{BGK}}[f] = \sum_{k_1 k_2 k_3} Q_{k_1 k_2 k_3}^{\text{BGK}} H^{k_1 k_2 k_3}(\mathbf{v}) \mathcal{M}(\mathbf{v}), \quad (3.1)$$

where

$$Q_{k_1 k_2 k_3}^{\text{BGK}} = \begin{cases} 0, & k_1 = k_2 = k_3 = 0, \\ -\frac{1}{7} f_{k_1 k_2 k_3}, & \text{otherwise.} \end{cases}$$

The expansions for the ES-BGK and Shakhov operators can be found in [6, 5]. In this section, we will first discuss the series expansion of the quadratic collision term  $\mathcal{Q}[f]$  defined in (2.2), and then mimic the BGK-type collision operators to construct collision models with better accuracy.

#### 3.1 Series expansions of general collision terms

Suppose the binary collision term  $\mathcal{Q}[f]$  can be expanded as

$$\mathcal{Q}[f](\mathbf{v}) = \sum_{k_1 k_2 k_3} Q_{k_1 k_2 k_3} H^{k_1 k_2 k_3}(\mathbf{v}) \mathcal{M}(\mathbf{v}). \quad (3.2)$$

By the orthogonality of Hermite polynomials, we get

$$Q_{k_1 k_2 k_3} = \frac{1}{k_1! k_2! k_3!} \int H^{k_1 k_2 k_3}(\mathbf{v}) \mathcal{Q}[f](\mathbf{v}) d\mathbf{v} = \sum_{i_1 i_2 i_3} \sum_{j_1 j_2 j_3} A_{k_1 k_2 k_3}^{i_1 i_2 i_3, j_1 j_2 j_3} f_{i_1 i_2 i_3} f_{j_1 j_2 j_3}, \quad (3.3)$$

where the second equality can be obtained by inserting (2.15) into (2.2), and

$$A_{k_1 k_2 k_3}^{i_1 i_2 i_3, j_1 j_2 j_3} = \frac{1}{(2\pi)^3 k_1! k_2! k_3!} \int_{\mathbb{R}^3} \int_{\mathbb{R}^3} \int_{\mathbf{n} \perp \mathbf{g}} \int_0^\pi B(|\mathbf{g}|, \chi) [H^{i_1 i_2 i_3}(\mathbf{v}') H^{j_1 j_2 j_3}(\mathbf{v}'_1) - H^{i_1 i_2 i_3}(\mathbf{v}) H^{j_1 j_2 j_3}(\mathbf{v}_1)] H^{k_1 k_2 k_3}(\mathbf{v}) \exp\left(-\frac{|\mathbf{v}|^2 + |\mathbf{v}_1|^2}{2}\right) d\chi d\mathbf{n} d\mathbf{v}_1 d\mathbf{v}. \quad (3.4)$$

It can be seen from (3.4) that the evaluation of every coefficient requires integration of an eight-dimensional function. In principle, this can be done by numerical quadrature; however, the computational cost for obtaining all these coefficients would be huge. Actually, in [21, 39], a strategy to simplify the above integral has been introduced, and for small indices, the values are given in the literature. However, when the indices are large, no explicit formulae are provided in [21, 39], and the procedure therein is not easy to follow. Inspired by these works, we give in this paper explicit equations of the coefficients  $A_{k_1 k_2 k_3}^{i_1 i_2 i_3, j_1 j_2 j_3}$  for any collision kernel, except for an integral with respect the two parameters in the kernel function  $B(\cdot, \cdot)$ . The main results are summarized in the following two theorems:

**Theorem 1.** *The expansion coefficients of the collision operator  $\mathcal{Q}[f](\mathbf{v})$  defined in (3.3) have the form below:*

$$A_{k_1 k_2 k_3}^{i_1 i_2 i_3, j_1 j_2 j_3} = \sum_{i'_1=0}^{\min(i_1+j_1, k_1)} \sum_{i'_2=0}^{\min(i_2+j_2, k_2)} \sum_{i'_3=0}^{\min(i_3+j_3, k_3)} \frac{2^{-k/2}}{2^3 \pi^{3/2} l'_1! l'_2! l'_3!} a_{i'_1 j'_1}^{i_1 j_1} a_{i'_2 j'_2}^{i_2 j_2} a_{i'_3 j'_3}^{i_3 j_3} \gamma_{j'_1 j'_2 j'_3}^{l'_1 l'_2 l'_3}, \quad (3.5)$$

where

$$j'_s = i_s + j_s - i'_s, \quad l'_s = k_s - i'_s, \quad s = 1, 2, 3. \quad (3.6)$$

The coefficients  $a_{i'j'}^{ij}$  and  $\gamma_{j_1 j_2 j_3}^{l_1 l_2 l_3}$  are defined by

$$a_{i'j'}^{ij} = 2^{-(i'+j')/2} i! j! \sum_{s=\max(0, i'-j)}^{\min(i', i)} \frac{(-1)^{j'-i+s}}{s!(i-s)!(i'-s)!(j'-i+s)!}, \quad (3.7)$$

and

$$\gamma_{j_1 j_2 j_3}^{l_1 l_2 l_3} := \int_{\mathbb{R}^3} \int_{\mathbf{n} \perp \mathbf{g}} \int_0^\pi \left[ H^{j_1 j_2 j_3} \left( \frac{\mathbf{g}'}{\sqrt{2}} \right) - H^{j_1 j_2 j_3} \left( \frac{\mathbf{g}}{\sqrt{2}} \right) \right] H^{l_1 l_2 l_3} \left( \frac{\mathbf{g}}{\sqrt{2}} \right) B(|\mathbf{g}|, \chi) \exp \left( -\frac{|\mathbf{g}|^2}{4} \right) d\chi d\mathbf{n} d\mathbf{g}, \quad (3.8)$$

where  $\mathbf{g}' = \mathbf{g} \cos \chi - |\mathbf{g}| \mathbf{n} \sin \chi$  is the post-collisional relative velocity, and  $B(|\mathbf{g}|, \chi)$  is the collision kernel in (2.2).

**Theorem 2.** For any  $k_1, k_2, k_3, l_1, l_2, l_3 \in \mathbb{N}$ , let  $k = k_1 + k_2 + k_3$  and  $l = l_1 + l_2 + l_3$ . Then the coefficients  $\gamma_{j_1 j_2 j_3}^{l_1 l_2 l_3}$  defined in (3.8) satisfies

$$\gamma_{k_1 k_2 k_3}^{l_1 l_2 l_3} = \sum_{m_1=0}^{\lfloor k_1/2 \rfloor} \sum_{m_2=0}^{\lfloor k_2/2 \rfloor} \sum_{m_3=0}^{\lfloor k_3/2 \rfloor} \sum_{n_1=0}^{\lfloor l_1/2 \rfloor} \sum_{n_2=0}^{\lfloor l_2/2 \rfloor} \sum_{n_3=0}^{\lfloor l_3/2 \rfloor} (2k-4m+1) C_{m_1 m_2 m_3}^{k_1 k_2 k_3} C_{n_1 n_2 n_3}^{l_1 l_2 l_3} S_{k_1-2m_1, k_2-2m_2, k_3-2m_3}^{l_1-2n_1, l_2-2n_2, l_3-2n_3} K^{kl}, \quad (3.9)$$

where  $m = m_1 + m_2 + m_3$ ,  $n = n_1 + n_2 + n_3$ , and

$$C_{m_1 m_2 m_3}^{k_1 k_2 k_3} = \frac{(-1)^m 4\pi m!}{(2(k-m)+1)!!} \frac{k_1! k_2! k_3!}{m_1! m_2! m_3!}. \quad (3.10)$$

In (3.9),  $S_{k_1 k_2 k_3}^{l_1 l_2 l_3}$  is the coefficient of  $v_1^{k_1} v_2^{k_2} v_3^{k_3} w_1^{l_1} w_2^{l_2} w_3^{l_3}$  in the polynomial

$$S_k(\mathbf{v}, \mathbf{w}) := (|\mathbf{v}| |\mathbf{w}|)^k P_k \left( \frac{\mathbf{v}}{|\mathbf{v}|} \cdot \frac{\mathbf{w}}{|\mathbf{w}|} \right), \quad (3.11)$$

and

$$K_{mn}^{kl} = \int_0^{+\infty} \int_0^\pi L_m^{(k-2m+1/2)} \left( \frac{g^2}{4} \right) L_n^{(l-2n+1/2)} \left( \frac{g^2}{4} \right) \times \left( \frac{g}{\sqrt{2}} \right)^{k+l+2-2(m+n)} B(g, \chi) \left[ P_{k-2m}(\cos \chi) - 1 \right] \exp \left( -\frac{g^2}{4} \right) d\chi dg. \quad (3.12)$$

Here  $L_n^{(\alpha)}(x)$  are the Laguerre polynomials and  $P_k(x)$  are the Legendre polynomials, which are defined below.

**Definition 2** (Legendre functions). For  $\ell \in \mathbb{N}$ , the Legendre polynomial  $P_\ell(x)$  is defined as

$$P_\ell(x) = \frac{1}{2^\ell \ell!} \frac{d^\ell}{dx^\ell} \left[ (x^2 - 1)^\ell \right].$$

**Definition 3** (Laguerre polynomials). For  $\alpha > -1$ , let  $w^\alpha(x) = x^{n+\alpha} \exp(-x)$ . For  $n \in \mathbb{N}$ , define the Laguerre polynomial as

$$L_n^{(\alpha)}(x) = \frac{x^n}{n! w^\alpha(x)} \frac{d^n}{dx^n} w^\alpha(x).$$

Through these two theorems, the eight-dimensional integration in (3.4) has been reduced into a series of summations and a two-dimensional integration. Among all the coefficients introduced in these theorems,  $a_{i'j'}^{ij}$  and  $C_{m_1 m_2 m_3}^{k_1 k_2 k_3}$  can be computed directly. As for  $S_{k_1 k_2 k_3}^{l_1 l_2 l_3}$ , we need to expand polynomial  $S_k(\mathbf{v}, \mathbf{w})$ , which can be done recursively using the following recursion formula:

$$\begin{aligned} S_0(\mathbf{v}, \mathbf{w}) &= 1, & S_1(\mathbf{v}, \mathbf{w}) &= \mathbf{v} \cdot \mathbf{w}, \\ S_{k+1}(\mathbf{v}, \mathbf{w}) &= \frac{2k+1}{k+1}(\mathbf{v} \cdot \mathbf{w})S_k(\mathbf{v}, \mathbf{w}) - \frac{k}{k+1}(|\mathbf{v}||\mathbf{w}|)^2 S_{k-1}(\mathbf{v}, \mathbf{w}). \end{aligned} \quad (3.13)$$

This recursion formula can be derived from the recursion relation of Legendre polynomials, and it also shows that for every monomial in the expansion of  $S_k(\mathbf{v}, \mathbf{w})$ , the degree of  $\mathbf{v}$  equals the degree of  $\mathbf{w}$ . Therefore  $S_{k_1 k_2 k_3}^{l_1 l_2 l_3}$  is nonzero only when  $k_1 + k_2 + k_3 = l_1 + l_2 + l_3$ . This means in (3.9), the summand is nonzero only when

$$k_1 + k_2 + k_3 - 2(m_1 + m_2 + m_3) = l_1 + l_2 + l_3 - 2(n_1 + n_2 + n_3). \quad (3.14)$$

Consequently, when evaluating  $K_{mn}^{kl}$  defined in (3.12), we only need to take into account the case  $k - 2m = l - 2n$ . Generally,  $K_{mn}^{kl}$  can be computed by numerical quadrature; for the IPL model, the integral with respect to  $g$  can be written explicitly, which will be elaborated in the following section.

### 3.2 Series expansion of collision operators for IPL models

The formulae given in the previous section are almost ready to be coded, except that specific collision models are needed to calculate the integral  $K_{mn}^{kl}$  defined in (3.12). This section is devoted to further simplifying this integral for IPL models, which completes the algorithm for computing the coefficients  $A_{k_1 k_2 k_3}^{i_1 i_2 i_3, j_1 j_2 j_3}$ .

For the IPL model (2.5), we first consider the integral with respect to  $\chi$  in (3.12). To this aim, we extract all the terms related to  $\chi$  from (3.12), and define  $\tilde{B}_k^\eta(\cdot)$  as

$$\tilde{B}_k^\eta(g) := \int_0^\pi B(g, \chi) [P_k(\cos \chi) - 1] d\chi = g^{\frac{\eta-5}{\eta-1}} \int_0^\pi W_0 \left| \frac{dW_0}{d\chi} \right| [P_k(\cos \chi) - 1] d\chi, \quad \eta > 3, \quad g > 0.$$

To evaluate the above integral, we follow the method introduced in [8] and apply the change of variable

$$\chi = \pi - 2 \int_0^1 [1 - x^2(1-y) - x^{\eta-1}y]^{-1/2} \sqrt{1-y} dx,$$

to get

$$\tilde{B}_k^\eta(g) = 2^{-\frac{\eta-3}{\eta-1}} g^{\frac{\eta-5}{\eta-1}} \int_0^1 [P_k(\cos \chi) - 1] [2(1-y) + (\eta-1)y]^{-(\eta-1)} dy, \quad (3.15)$$

Below we write the above equation as

$$\tilde{B}_k^\eta(g) = 2^{-\frac{\eta-3}{\eta-1}} g^{\frac{\eta-5}{\eta-1}} \mathcal{I}(k, \eta), \quad (3.16)$$

where  $\mathcal{I}(k, \eta)$  denotes the integral in (3.15). In general, we need to evaluate  $\mathcal{I}(k, \eta)$  by numerical quadrature. In our implementation, the adaptive integrator introduced in [36, Section 3.3.7] is used to compute this integral.

Now we consider the integral with respect to  $g$ . Using the result (3.16), we can rewrite (3.12) as

$$K_{mn}^{kl} = 2^{c(\eta)} \mathcal{I}(k-2m, \eta) \int_0^{+\infty} L_m^{(k-2m+1/2)}(s) L_n^{(k-2m+1/2)}(s) s^{c(\eta)} \exp(-s) ds, \quad (3.17)$$

where  $c(\eta) = \frac{\eta-3}{\eta-1} + k - 2m$ , and we have applied the change of variable  $s = g^2/4$ , and taken into account the relation  $k - 2m = l - 2n$ . In general, we can adopt the formula

$$\int_0^{+\infty} L_m^{(\alpha)}(s) L_n^{(\alpha)}(s) s^\mu \exp(-s) ds = (-1)^{m+n} \Gamma(\mu+1) \sum_{i=0}^{\min(m,n)} \binom{\mu-\alpha}{m-i} \binom{\mu-\alpha}{n-i} \binom{i+\mu}{i} \quad (3.18)$$

introduced in [38, eq. (10)] to calculate (3.17). Specially, when  $\eta = 5$ , which corresponds to the model of Maxwell molecules, we can use the orthogonality of Laguerre polynomials to get

$$K_{mn}^{kl} = 2^{k-2m+1/2} \mathcal{I}(k-2m, 5) \binom{k-m+1/2}{m} \Gamma(k-2m+3/2) \delta_{mn}, \quad (3.19)$$

and thus the computational cost can be further reduced. In fact, Grad has already pointed out in [21] that for Maxwell molecules,  $A_{k_1 k_2 k_3}^{i_1 i_2 i_3, j_1 j_2 j_3}$  is nonzero only when

$$i_1 + i_2 + i_3 + j_1 + j_2 + j_3 = k_1 + k_2 + k_3. \quad (3.20)$$

This can also be seen from our calculation: from (3.19), we can find that only when  $k_1 + k_2 + k_3 = l_1 + l_2 + l_3$ , the coefficient  $\gamma_{k_1 k_2 k_3}^{l_1 l_2 l_3}$  given in (3.9) is nonzero; therefore in (3.5), if the summand is nonzero, the sum of  $j'_1, j'_2$  and  $j'_3$  must equal the sum of  $l'_1, l'_2$  and  $l'_3$ , which is equivalent to (3.20) due to (3.6).

The above analysis shows that for the IPL model, we only need to apply the numerical quadrature to the one-dimensional integrals  $\mathcal{I}(k, \eta)$ , which makes it easier to obtain the coefficients  $A_{k_1 k_2 k_3}^{i_1 i_2 i_3, j_1 j_2 j_3}$  with high accuracy.

### 3.3 Approximation of the collision term

Until now, we already have a complete algorithm to calculate the coefficients  $A_{k_1 k_2 k_3}^{i_1 i_2 i_3, j_1 j_2 j_3}$ . These coefficients can be used either to discretize the collision term or to construct new collision models. We will discuss both topics in this section.

#### 3.3.1 Discretization of the homogeneous Boltzmann equation

Based on the expansion of the distribution function (2.15), the most natural discretization of the homogeneous Boltzmann equation is to use the Galerkin spectral method. From this point of view, for any positive integer  $M$ , we define the space of the numerical solution

$$\mathcal{F}_M = \text{span}\{H^{k_1 k_2 k_3}(\mathbf{v}) \mathcal{M}(\mathbf{v}) \mid (k_1, k_2, k_3) \in I_M\} \subset \mathcal{F} = L^2(\mathbb{R}^3; \mathcal{M}^{-1} d\mathbf{v}), \quad (3.21)$$

where  $I_M$  is the index set

$$I_M = \{(k_1, k_2, k_3) \mid 0 \leq k_1 + k_2 + k_3 \leq M, k_i \in \mathbb{N}, i = 1, 2, 3\}.$$

Then the semi-discrete distribution function  $f_M(t, \cdot) \in \mathcal{F}_M$  satisfies

$$\int_{\mathbb{R}^3} \frac{\partial f_M}{\partial t} \varphi \mathcal{M}^{-1} d\mathbf{v} = \int_{\mathbb{R}^3} \mathcal{Q}(f_M, f_M) \varphi \mathcal{M}^{-1} d\mathbf{v}, \quad \forall \varphi \in \mathcal{F}_M. \quad (3.22)$$

Suppose

$$f_M(t, \mathbf{v}) = \sum_{(k_1, k_2, k_3) \in I_M} f_{k_1 k_2 k_3}(t) H^{k_1 k_2 k_3}(\mathbf{v}) \mathcal{M}(\mathbf{v}) \in \mathcal{F}_M. \quad (3.23)$$

The equations (3.2) and (3.3) show that the variational form (3.22) is equivalent to the following ODE system:

$$\frac{df_{k_1 k_2 k_3}}{dt} = \sum_{(i_1, i_2, i_3) \in I_M} \sum_{(j_1, j_2, j_3) \in I_M} A_{k_1 k_2 k_3}^{i_1 i_2 i_3, j_1 j_2 j_3} f_{i_1 i_2 i_3} f_{j_1 j_2 j_3}, \quad (k_1, k_2, k_3) \in I_M. \quad (3.24)$$

It is easy to see that the time complexity for the computation of all the right-hand sides is proportional to the number of nonzero coefficients. For most collision operators, the coefficients  $A_{k_1 k_2 k_3}^{i_1 i_2 i_3, j_1 j_2 j_3}$  form a full tensor, since there is no evidence showing that  $A_{k_1 k_2 k_3}^{i_1 i_2 i_3, j_1 j_2 j_3}$  can be zero, except a few coefficients related to the conservation laws. Therefore, the computational cost for the right-hand side of (3.24) is  $O(N_M^3) = O(M^9)$ , where  $N_M$  is the number of elements in  $I_M$ :

$$N_M = \frac{(M+1)(M+2)(M+3)}{6} \sim O(M^3). \quad (3.25)$$

However, when considering Maxwell molecules, due to the constraint (3.20), the computational cost can be reduced to  $O(M^8)$ .

To fully formulate the ODE system (3.24), we need the coefficients  $A_{k_1 k_2 k_3}^{i_1 i_2 i_3, j_1 j_2 j_3}$  for all  $(i_1, i_2, i_3), (j_1, j_2, j_3), (k_1, k_2, k_3) \in I_M$ . When the collision kernel is chosen and  $M$  is fixed, we only need to compute these coefficients once, and then they can be used repeatedly. For a given  $M$ , the algorithm for computing these coefficients is summarized in Table 1. The general procedure is to sequentially compute the coefficients in the first column, with indices described in the third column, and the equations to follow are given in the second column. For IPL models, we can use (3.17) and (3.18) instead to obtain the values of  $K_{mn}^{kl}$ . In the third column of Table 1, it is worth mentioning that some indices are in the index set  $I_{2M}$  instead of  $I_M$ , as is due to the equation (3.6), which shows that

$$(j'_1, j'_2, j'_3) \in I_{2M}, \quad \text{if } (i_1, i_2, i_3) \in I_M \text{ and } (j_1, j_2, j_3) \in I_M.$$

Therefore the corresponding indices for  $\gamma$  and  $C$  must lie in  $I_{2M}$ . Similar arguments hold for the coefficients  $K$ .

The last column in Table 1 shows an estimation of the computational cost for each coefficient, from which one can see that the total cost for getting  $A_{k_1 k_2 k_3}^{i_1 i_2 i_3, j_1 j_2 j_3}$  is  $O(M^{12})$ . Now we compare this with the numerical cost by applying numerical integration directly to (3.4). We assume the number of quadrature points on  $\mathbb{R}^3$  is  $O(M_v^3)$ , and the number of quadrature points on the unit sphere (domain for  $\mathbf{n}$  and  $\chi$ ) is  $O(M_s^2)$ . Thus using numerical integration to evaluate all the coefficients  $A_{k_1 k_2 k_3}^{i_1 i_2 i_3, j_1 j_2 j_3}$  has time complexity  $O(M^9 M_v^6 M_s^2)$ . In most cases, we will choose  $M_v > M$  to get accurate results. Hence our method listed in Table 1 is significantly faster.

### 3.3.2 Approximation of the collision operator

In the previous section, a complete numerical method has been given to solve the spatially homogeneous Boltzmann equation. However, due to the rapid growth of the number of coefficients as  $M$  increases, the storage requirement of this algorithm is quite strong. Table 2 shows the memory required to store the coefficients  $A_{k_1 k_2 k_3}^{i_1 i_2 i_3, j_1 j_2 j_3}$ , where we assume that the coefficients are represented in the double-precision floating-point format, whose typical size is 8 bytes per

Coefficients	Formula	Constraints for the indices	Computational cost
$C_{m_1 m_2 m_3}^{k_1 k_2 k_3}$	(3.10)	$(k_1, k_2, k_3) \in I_{2M}, (m_1, m_2, m_3) \in I_M$	$O(M^6)$
$S_{l_1 l_2 l_3}^{k_1 k_2 k_3}$	(3.13)	$(k_1, k_2, k_3) \in I_M, (l_1, l_2, l_3) \in I_M, k_1 + k_2 + k_3 = l_1 + l_2 + l_3$	$O(M^5)$
$K_{mn}^{kl}$	(3.12)	$k \leq 2M, l \leq M, m \leq \lfloor k/2 \rfloor, n \leq \lfloor l/2 \rfloor, k - 2m = l - 2n$	$O(M^4)$
$\gamma_{k_1 k_2 k_3}^{l_1 l_2 l_3}$	(3.9)	$(l_1, l_2, l_3) \in I_M, (k_1, k_2, k_3) \in I_{2M}$	$O(M^{11})$
$a_{i' j'}^{ij}$	(3.7)	$i \leq M, j \leq M, i' \leq 2M, j' \leq 2M, i + j = i' + j'$	$O(M^4)$
$A_{k_1 k_2 k_3}^{i_1 i_2 i_3, j_1 j_2 j_3}$	(3.5)	$(k_1, k_2, k_3) \in I_M, (i_1, i_2, i_3) \in I_M, (j_1, j_2, j_3) \in I_M$	$O(M^{12})$

Table 1: A summary for computation of all the coefficients.

number. It can be seen that the case  $M = 20$  has already exceeded the memory caps of most current desktops. Although the data given in Table 2 can be reduced by taking the symmetry of the coefficients into consideration, it can still easily hit our memory limit by increasing  $M$  slightly. Even if the memory cost is acceptable for large  $M$ , the computational cost  $O(M^9)$  becomes an issue especially when solving the spatially inhomogeneous problems.

$M$	Memory (Gigabytes)	$M$	Memory (Gigabytes)
5	$1.308 \times 10^{-3}$	25	$2.620 \times 10^2$
10	0.1743	30	$1.210 \times 10^3$
15	4.048	35	$4.473 \times 10^3$
20	41.38	40	$1.400 \times 10^4$

Table 2: Memory required to store  $A_{k_1 k_2 k_3}^{i_1 i_2 i_3, j_1 j_2 j_3}$ .

To overcome this difficulty, we will only compute and store the coefficients  $A_{k_1 k_2 k_3}^{i_1 i_2 i_3, j_1 j_2 j_3}$  for a small number  $M$  such that the computational cost for solving (3.24) is acceptable. When  $(k_1, k_2, k_3) \notin I_M$ , we apply the idea of the BGK-type models and let these coefficients decay to zero exponentially with a constant rate:

$$\frac{df_{k_1 k_2 k_3}}{dt} = -\nu_M f_{k_1 k_2 k_3}, \quad (k_1, k_2, k_3) \notin I_M, \quad (3.26)$$

where  $\nu_M$  is a constant independent of  $k_1, k_2$  and  $k_3$ . Combining (3.24) and (3.26), we actually get a new collision operator

$$\mathcal{Q}_M[f] = P_M \mathcal{Q}[P_M f] - \nu_M (I - P_M) f, \quad \forall f \in \mathcal{F}, \quad (3.27)$$

where  $P_M$  is the orthogonal projection from  $\mathcal{F}$  onto  $\mathcal{F}_M$ . Such a idea is to mimic the derivation of Shakhov model [37], which models the collision by

$$\mathcal{Q}^S[f] := P_{G13} \mathcal{L}[P_{G13} f] - \nu (I - P_{G13}) f, \quad \forall f \in \mathcal{F}, \quad (3.28)$$

where  $\mathcal{L}$  is the linearized collision operator defined by

$$\mathcal{L}[f] := \lim_{\epsilon \rightarrow 0} \frac{Q[\mathcal{M} + \epsilon(f - \mathcal{M})]}{\epsilon}$$

and  $P_{G13}$  is the projection operator onto the 13-dimensional subspace

$$\mathcal{F}_{G13} = \left\{ p(\mathbf{v}) \mathcal{M}(\mathbf{v}) \left| p(\mathbf{v}) = \alpha + \sum_{j=1}^3 \beta_j v_j + \sum_{i,j=1}^3 \gamma_{ij} v_i v_j + \sum_{j=1}^3 \zeta_j |\mathbf{v}|^2 v_j \right. \right\}$$

which includes Grad's 13 moments [21]. Comparing (3.27) and (3.28), one finds that in our model, we have replaced the linearized collision operator  $\mathcal{L}$  by the more accurate quadratic collision operator  $\mathcal{Q}$ , and the subspace  $\mathcal{F}_{G13}$  is replaced by the larger space  $\mathcal{F}_M$  once  $M \geq 3$ . Thus the proposed model is expected to provide better accuracy than the Shakhov model.

The difference between the proposed model and the original quadratic model is to be further studied in the future work. In general, we suppose

1. The projection operator  $P_M$  has spectral accuracy;
2.  $\mathcal{Q}[P_M f]$  approximates  $\mathcal{Q}[f]$  with spectral accuracy.

Then

$$\|\mathcal{Q}_M[f] - \mathcal{Q}[f]\| \leq \|P_M \mathcal{Q}[P_M f] - \mathcal{Q}[P_M f]\| + \|\mathcal{Q}[P_M f] - \mathcal{Q}[f]\| + |\nu_M| \|f - P_M f\|,$$

from which one can see that  $\mathcal{Q}^S[f]$  approximates  $\mathcal{Q}[f]$  with spectral accuracy. Applying spectral method to this collision operator is quite straightforward. One just needs to choose an appropriate  $M$  (modelling parameter) and an appropriate index set for  $k_1, k_2$  and  $k_3$  (discretization parameter), and then solve the ODE system combined by (3.24) and (3.26) for  $k_1, k_2, k_3$  in the index set. Thus, it remains only to select the constant  $\nu_M$ .

In [8], the authors used a similar idea to approximate the linearized collision operator, where the evolution of the coefficients for high-degree basis functions is also approximated by an exponential decay. Here we choose the decay rate in the same way as in [8]: considering the discrete linearized collision operator  $\mathcal{L}_M : \mathcal{F}_M \rightarrow \mathcal{F}_M$  defined as

$$\mathcal{L}_M[f] = \sum_{(k_1, k_2, k_3) \in I_M} \sum_{(j_1, j_2, j_3) \in I_M} (A_{k_1 k_2 k_3}^{000, j_1 j_2 j_3} + A_{k_1 k_2 k_3}^{j_1 j_2 j_3, 000}) f_{j_1 j_2 j_3} H^{k_1 k_2 k_3}(\mathbf{v}) \mathcal{M}(\mathbf{v}), \quad (3.29)$$

we let  $\nu_M$  be the spectral radius of this operator. The idea of such a choice includes the following:

1. As "less important coefficients" ( $(k_1, k_2, k_3) \notin I_M$ ), the decay rate should be faster than all the "important coefficients" ( $(k_1, k_2, k_3) \in I_M$ ). Therefore we choose  $\nu_M \geq \rho(\mathcal{L}_M)$ , where  $\rho(\mathcal{L}_M)$  is the spectral radius of  $\mathcal{L}_M$ , indicating the fastest decay rate for the important coefficients.
2. We do not want to introduce any gap between the spectrum of the two parts, causing a sharp transition in the frequency space. Therefore we choose  $\nu_M = \rho(\mathcal{L}_M)$ .

Additionally, it has also been shown in [8] that such a choice of  $\nu_M$  agrees with the choice of  $\nu$  in the Shakhov model (3.28). By taking the same  $\nu_M$  in  $\mathcal{Q}_M[f]$ , the linearization of  $\mathcal{Q}_M[f]$  about the Maxwellian  $\mathcal{M}$  coincides with the approximation of the linearized collision operator proposed in [8].

The collision operator  $\mathcal{Q}_M$  deals with a high-frequency modes with a very simple method: they are damped to zero at a uniform decay rate. However, in the solution of the Boltzmann equation, it is often observed that higher-frequency modes decay faster (see Section 4.1 for an example). This can be achieved by a more careful modelling for the higher-frequency modes. Although not yet implemented, we would like to discuss some possibilities to make improvements. The first possibility is to replace the simple uniform decay by the linearized collision operator:

$$\mathcal{Q}_M^*[f] = P_M \mathcal{Q}[P_M f] + \mathcal{L}[(I - P_M)f].$$

Since the computation of the linearized collision operator is much cheaper than that of the quadratic collision operator [8], it can be expected that such a method can provide a quite



accurate approximation when the computational cost of the linearized collision operator is acceptable. Another possibility is to give each coefficient a different decay rate:

$$\mathcal{Q}_M^{**}[f](\mathbf{v}) = P_M \mathcal{Q}[P_M f](\mathbf{v}) - \sum_{k_1+k_2+k_3>M} \nu_M^{k_1 k_2 k_3} f_{k_1 k_2 k_3} H^{k_1 k_2 k_3}(\mathbf{v}) \mathcal{M}(\mathbf{v}),$$

and a possible choice of  $\nu_M^{k_1 k_2 k_3}$  is the corresponding term in the linearized collision operator:

$$\nu_M^{k_1 k_2 k_3} = -\frac{1}{k_1! k_2! k_3!} \int_{\mathbb{R}^3} \mathcal{L}[\varphi^{k_1 k_2 k_3}](\mathbf{v}) H^{k_1 k_2 k_3}(\mathbf{v}) d\mathbf{v},$$

where  $\varphi^{k_1 k_2 k_3}(\mathbf{v}) = H^{k_1 k_2 k_3}(\mathbf{v}) \mathcal{M}(\mathbf{v})$  is the basis function. The effect of these finer approximations will be studied in the future work.

By now, we have obtained a series of new collision models (3.27). It can be expected that these models are better approximations of the original quadratic operator than the simple BGK-type models, especially when the non-equilibrium is strong and the non-linearity takes effect. This will be observed in the numerical examples.

## 4 Numerical examples

In this section, we will show some results of our numerical simulation. In all the numerical experiments, we adopt the newly proposed collision operator (3.27), and solve the equation

$$\frac{\partial f}{\partial t} = \mathcal{Q}_{M_0}[f]$$

numerically for some positive integer  $M_0$ . This equation is solved by the Galerkin spectral method with solution defined in the space  $\mathcal{F}_M$ , and  $M$  is always chosen to be greater than  $M_0$ . For the time discretization, we use the classical 4th-order Runge-Kutta method in all the examples, and the time step is chosen as  $\Delta t = 0.01$ .

### 4.1 BKW solution

For the Maxwell gas  $\eta = 5$ , the original spatially homogeneous Boltzmann equation (2.8) admits an exact solution with explicit expression:

$$f(t, \mathbf{v}) = (2\pi\tau(t))^{-3/2} \exp\left(-\frac{|\mathbf{v}|^2}{2\tau(t)}\right) \left[1 + \frac{1-\tau(t)}{\tau(t)} \left(\frac{|\mathbf{v}|^2}{2\tau(t)} - \frac{3}{2}\right)\right],$$

where  $\tau(t) = 1 - \exp\left(\frac{\pi}{3} \tilde{B}_2^5(t + t_0)\right)$ . In order that  $f(\mathbf{v}) \geq 0$  for all  $t \in \mathbb{R}_+$  and  $\mathbf{v} \in \mathbb{R}^3$ , the parameter  $t_0$  must satisfy

$$-\frac{\pi}{3} \tilde{B}_2^5 t_0 \geq \log\left(\frac{5}{2}\right) \approx 0.916291. \quad (4.1)$$

Here we choose  $t_0$  such that the left hand side of (4.1) equals to 0.92. To ensure a good approximation of the initial distribution function, we use  $M = 20$  (1771 degrees of freedom) in our simulation. For visualization purpose, we define the marginal distribution functions (MDFs)

$$g(t, v_1) = \int_{\mathbb{R}} f(t, \mathbf{v}) dv_2 dv_3, \quad h(t, v_1, v_2) = \int_{\mathbb{R}} f(t, \mathbf{v}) dv_3.$$

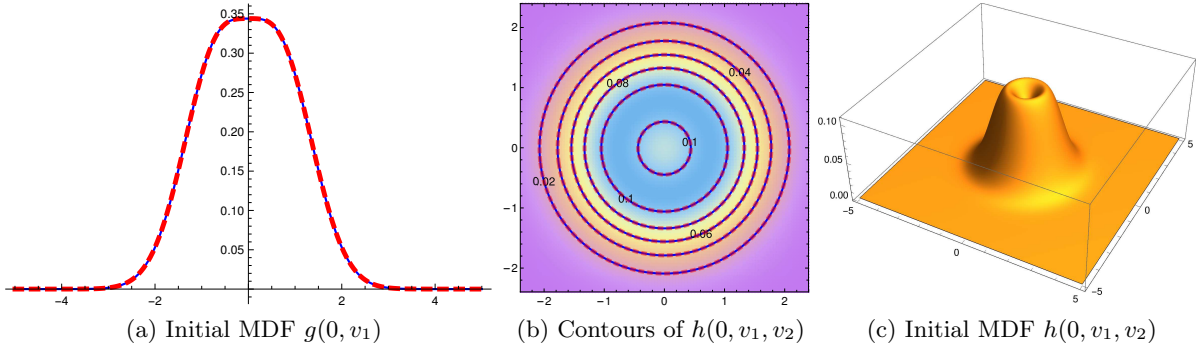


Figure 1: Initial marginal distribution functions. In (a) and (b), the blue solid lines correspond to the exact solution, and the red dashed lines correspond to the numerical approximation. Figure (c) shows only the numerical approximation.

The initial MDFs are plotted in Figure 1, in which the lines for exact functions and their numerical approximation are hardly distinguishable.

Numerical results for  $t = 0.2, 0.4$  and  $0.6$  are given in Figures 2 and 3, respectively for  $M_0 = 5$  and  $M_0 = 10$ . For  $M_0 = 5$ , the numerical solution provides a reasonable approximation, but still with noticeable deviations, while for  $M_0 = 10$ , the two solutions match perfectly in all cases. To study the computational time, we run the simulation for  $M_0 = 3, \dots, 12$  until  $t = 5$  on a single CPU core with model Intel<sup>®</sup> Core<sup>™</sup> i7-7600U. The relation between the computational time and the value of  $M_0$  is plotted in Figure 4. It can be seen that when  $M_0$  is large, the computational time is roughly proportional to the cube of the number of degrees of freedom. Note that the computational time also includes the time for processing the coefficients of basis functions with degree between  $M_0 + 1$  and  $M$ . Although the time complexity is only linear, when  $M_0$  is small, the number of such coefficients is quite large, and they have a significant contribution to the total computational time. This explains why the curve in Figure 4 decreases fast for the first few points. As a reference, we provide the average computational time for a single collision operator in Table 3.

$M_0$	3	4	5	6	7	8	9	10	11	12
Time (ms)	0.128	0.479	0.734	1.535	3.553	8.037	17.554	36.643	72.666	135.955

Table 3: Average computational time for a single collision operator for different values of  $M_0$ .

In Table 4, we provide the  $L^2$  and weighted  $L^2$  error of the numerical solutions at  $t = 0.5$  and  $t = 1.0$ . The notations in the table are

$$E_M^{(1)} = \left( \int_{\mathbb{R}^3} |f_{\text{num}}(\mathbf{v}) - f_{\text{exact}}(\mathbf{v})|^2 d\mathbf{v} \right)^{1/2}, \quad E_M^{(2)} = \left( \int_{\mathbb{R}^3} |f_{\text{num}}(\mathbf{v}) - f_{\text{exact}}(\mathbf{v})|^2 [\mathcal{M}(\mathbf{v})]^{-1} d\mathbf{v} \right)^{1/2},$$

where  $f_{\text{num}}$  is the numerical solution, and  $f_{\text{exact}}$  is the exact solution. Four different choices of  $M_0$  ( $M_0 = 5, 10, 15, 20$ ) and two different choices of  $M$  ( $M = M_0$  and  $M = 20$ ) are considered, from which we can see a rapid drop of the numerical error as  $M_0$  increases, indicating the spectral accuracy. When  $M_0 < 20$ , the results for  $M = 20$  are slightly more accurate than the corresponding results for  $M = M_0$ , especially when  $M_0$  is small. We expect that such a property is useful when simulating spatially inhomogeneous problems, for which the value of  $M_0$  cannot be too large due to the presence of the spatial variables.

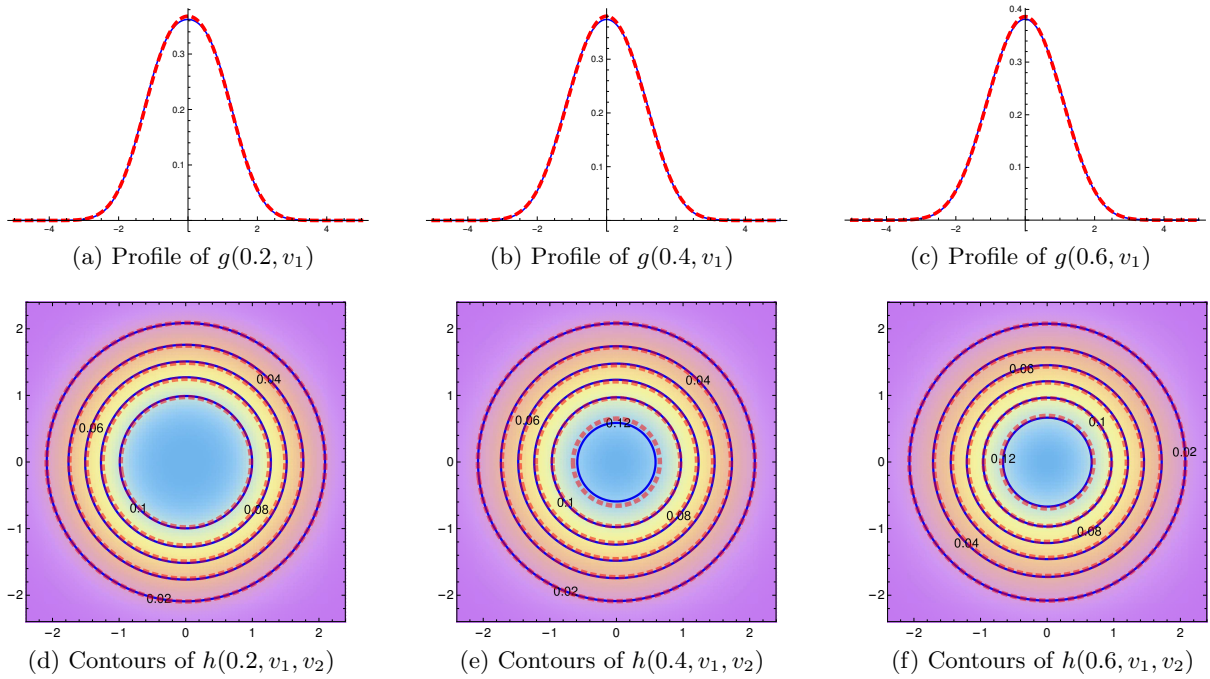


Figure 2: Marginal distribution functions for  $M_0 = 5$  at  $t = 0.2, 0.4$  and  $0.6$ . The blue lines correspond to the exact solution, and the red lines correspond to the numerical solutions.

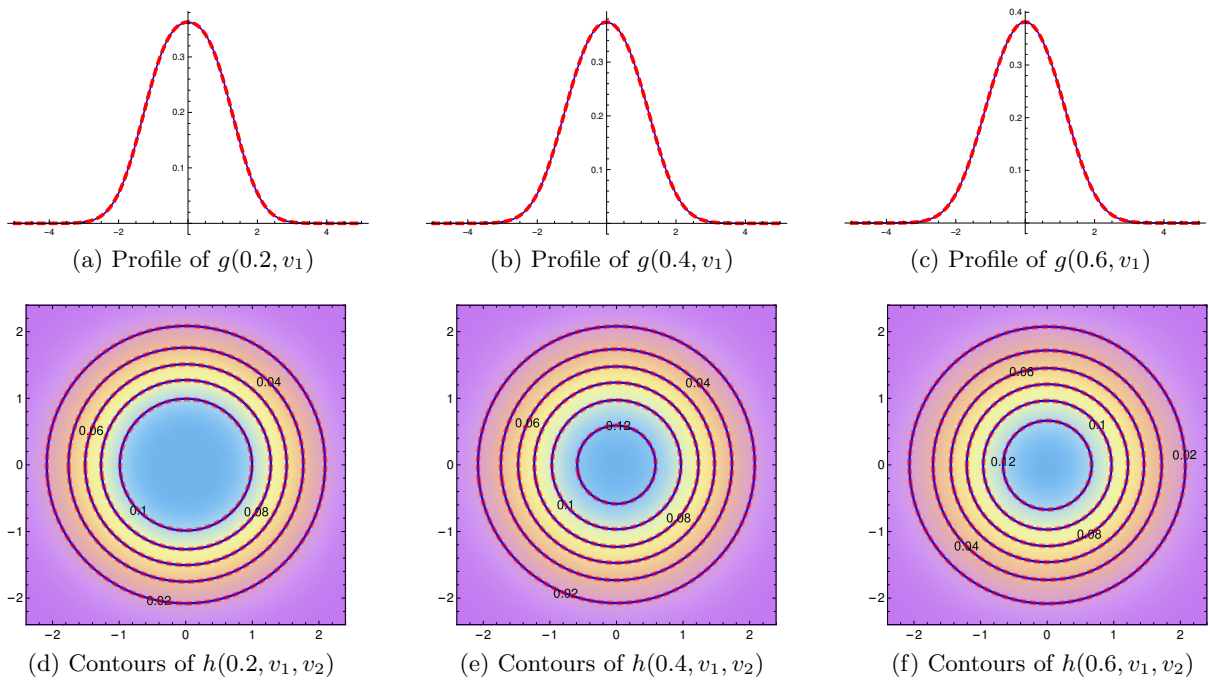


Figure 3: Marginal distribution functions for  $M_0 = 10$  at  $t = 0.2, 0.4$  and  $0.6$ . The blue lines correspond to the exact solution, and the red lines correspond to the numerical solutions.

Now we consider the time evolution of the moments. By expanding the exact solution into

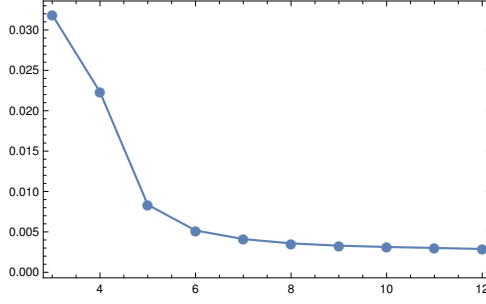


Figure 4: The horizontal axis is the value of  $M_0$ , and the vertical axis is the value of  $T_{M_0}/N_{M_0}^3$ , where  $T_{M_0}$  is the computational time (in milliseconds) for given  $M_0$  and  $N_{M_0}$  is defined in (3.25).

$M_0$	$t = 0.5$				$t = 1.0$			
	5	10	15	20	5	10	15	20
$E_{M_0}^{(1)}$	$1.04 \times 10^{-2}$	$5.40 \times 10^{-4}$	$5.94 \times 10^{-5}$	$1.90 \times 10^{-6}$	$3.19 \times 10^{-3}$	$6.09 \times 10^{-5}$	$3.40 \times 10^{-6}$	$3.89 \times 10^{-8}$
$E_{M_0}^{(2)}$	$7.46 \times 10^{-2}$	$4.69 \times 10^{-3}$	$5.57 \times 10^{-4}$	$1.93 \times 10^{-5}$	$2.52 \times 10^{-2}$	$5.90 \times 10^{-4}$	$3.50 \times 10^{-5}$	$4.32 \times 10^{-7}$
$E_{20}^{(1)}$	$6.48 \times 10^{-3}$	$3.71 \times 10^{-4}$	$4.49 \times 10^{-5}$	$1.90 \times 10^{-6}$	$2.78 \times 10^{-3}$	$5.53 \times 10^{-5}$	$3.20 \times 10^{-6}$	$3.89 \times 10^{-8}$
$E_{20}^{(2)}$	$5.05 \times 10^{-2}$	$3.42 \times 10^{-3}$	$4.31 \times 10^{-4}$	$1.93 \times 10^{-5}$	$2.28 \times 10^{-2}$	$5.40 \times 10^{-4}$	$3.31 \times 10^{-5}$	$4.32 \times 10^{-7}$

Table 4: Numerical error for the BKW solution.  $E_M^{(1)}$  is the  $L^2$  error, and  $E_M^{(2)}$  is the weighted  $L^2$  error. See text for details.

Hermite series, we get the exact solution for the coefficients:

$$f_{k_1 k_2 k_3}(t) = \begin{cases} \left[ -\frac{1}{2} \exp\left(\frac{\pi}{3} \tilde{B}_2^\eta(t+t_0)\right) \right]^{\frac{k_1+k_2+k_3}{2}} \frac{1 - (k_1 + k_2 + k_3)/2}{(k_1/2)!(k_2/2)!(k_3/2)!}, & \text{if } k_1, k_2, k_3 \text{ are even,} \\ 0, & \text{otherwise.} \end{cases}$$

This exact solution can also be written in terms of initial conditions as

$$f_{k_1 k_2 k_3}(t) = f_{k_1 k_2 k_3}(0) \exp\left(\frac{\pi}{6} \tilde{B}_2^\eta(k_1 + k_2 + k_3)t\right),$$

from which one can clearly see that coefficients for higher-degree polynomials decay faster, showing that a better modeling of the ‘‘BGK part’’ may yield better results. Due to the symmetry of the distribution function, the coefficients  $f_{k_1 k_2 k_3}$  are zero for any  $t$  if  $1 \leq k_1 + k_2 + k_3 \leq 3$ . Hence we will focus on the coefficients  $f_{400}$  and  $f_{220}$ , which are the fourth moments of the distribution function. For Maxwell molecules, the discrete kernel  $A_{k_1 k_2 k_3}^{l_1 l_2 l_3 m_1 m_2 m_3}$  is nonzero when  $k_1 + k_2 + k_3 = l_1 + l_2 + l_3 + m_1 + m_2 + m_3$ . Therefore, for any  $M \geq M_0 \geq 4$ , the numerical results for these two coefficients  $f_{400}$  and  $f_{220}$  are exactly the same (regardless of round-off errors). Figure 5 gives the comparison between the numerical solution and the exact solution for these two coefficients. In both plots, the two lines almost coincide with each other.

## 4.2 Bi-Gaussian initial data

In this example, we perform the numerical test for hard potential  $\eta = 10$ . The initial distribution function is

$$f(0, \mathbf{v}) = \frac{1}{2\pi^{3/2}} \left[ \exp\left(- (v_1 + \sqrt{3/2})^2 + v_2^2 + v_3^2\right) + \exp\left(- (v_1 - \sqrt{3/2})^2 + v_2^2 + v_3^2\right) \right].$$

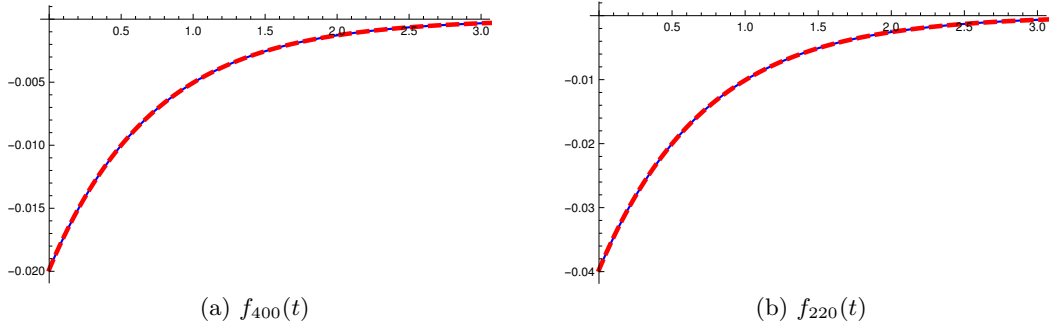


Figure 5: The evolution of the coefficients. The blue lines correspond to the reference solution, and the red lines correspond to the numerical solution.

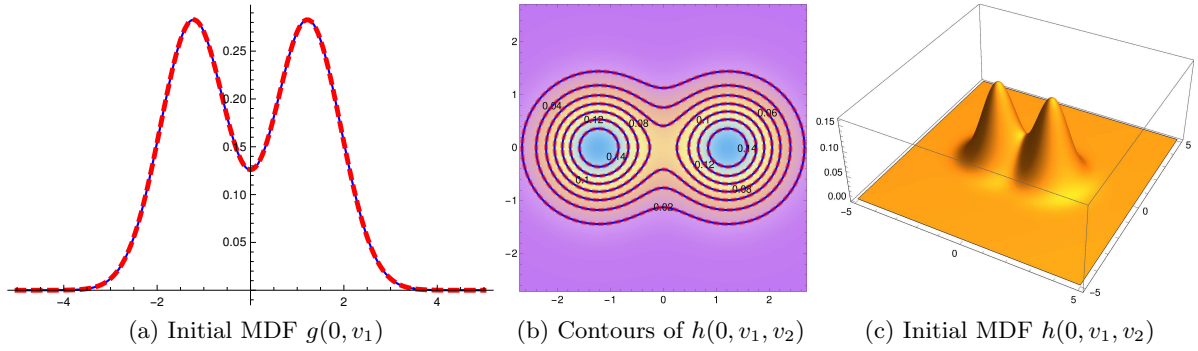


Figure 6: Initial marginal distribution functions. In (a) and (b), the blue solid lines correspond to the exact solution, and the red dashed lines correspond to the numerical approximation. Figure (c) shows only the numerical approximation.

Again, in all our numerical tests, we use  $M = 20$  which gives a good approximation of the initial distribution function (see Figure 6).

For this example, we consider the three cases  $M_0 = 5, 10, 15$ , and the corresponding one-dimensional marginal distribution functions at  $t = 0.3, 0.6$  and  $0.9$  are given in Figure 7. In all the results, the lines for  $M_0 = 10$  and  $M_0 = 15$  are very close to each other. Due to the fast convergence of the spectral method, it is believable that  $M_0 = 10$  can already provide a very good approximation. To get a clearer picture, similar comparison of two-dimensional results are also provided in Figure 8 and 9.

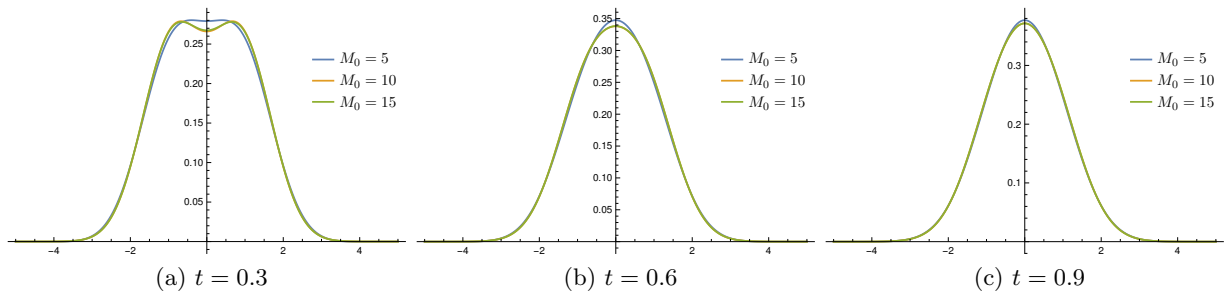


Figure 7: Marginal distribution functions at different times.

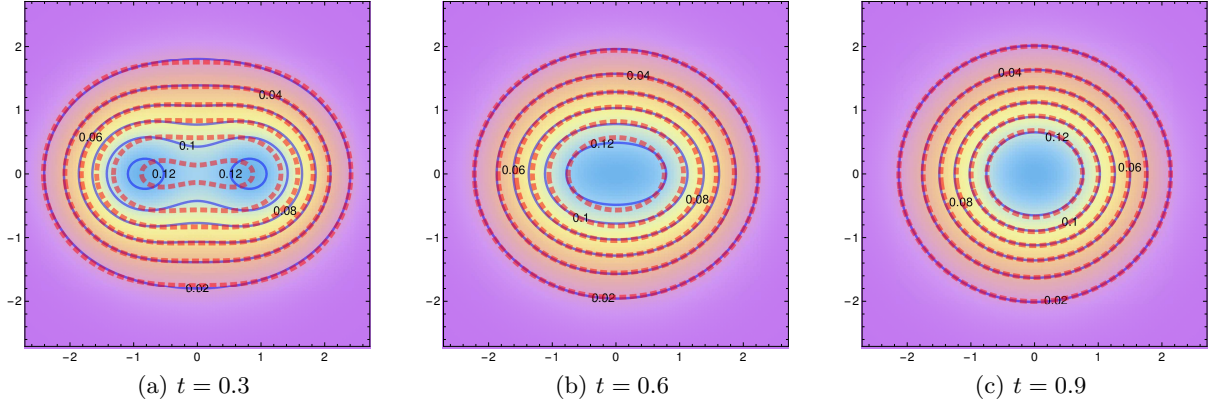


Figure 8: Comparison of numerical results using  $M_0 = 5$  and  $M_0 = 15$ . The blue contours and the red dashed contours are respectively the results for  $M_0 = 5$  and  $M_0 = 15$ .

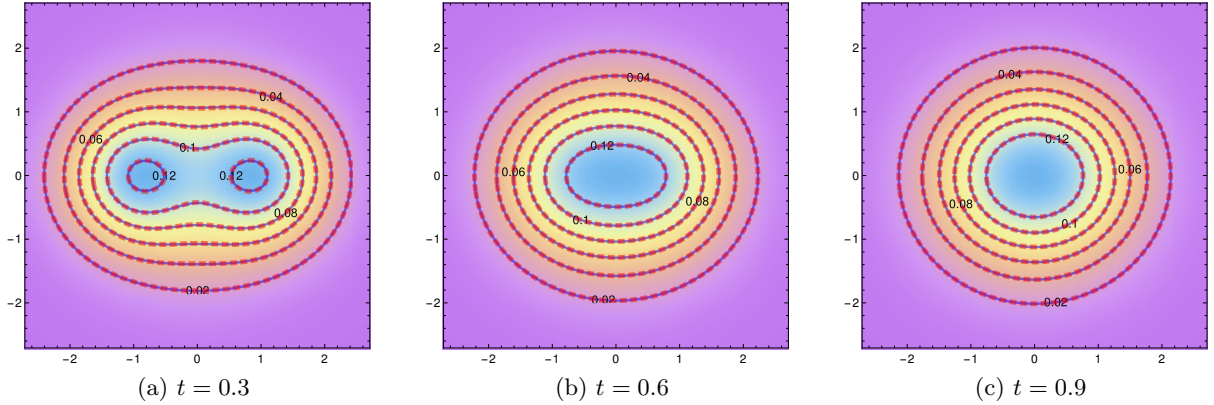


Figure 9: Comparison of numerical results using  $M_0 = 10$  and  $M_0 = 15$ . The blue contours and the red dashed contours are respectively the results for  $M_0 = 10$  and  $M_0 = 15$ .

Now we consider the evolution of the moments. In this example, we always have  $\sigma_{11} = -2\sigma_{22} = -2\sigma_{33}$  and  $q_1 = q_2 = q_3 = 0$ . Therefore we focus only on the evolution of  $\sigma_{11}$ , which is plotted in Figure 10. It can be seen that three tests give almost identical results. Even for  $M_0 = 5$ , while the distribution function is not approximated very well, the evolution of the stress tensor is almost exact.

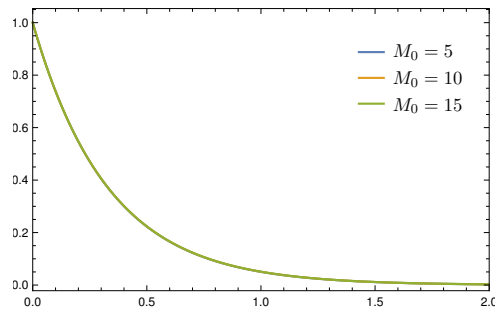


Figure 10: Evolution of  $\sigma_{11}(t)$ . Three lines are on top of each other.



### 4.3 Discontinuous initial data

Here we consider the problem with a discontinuous initial condition:

$$f(0, \mathbf{v}) = \begin{cases} \frac{\sqrt[4]{2}(2 - \sqrt{2})}{\pi^{3/2}} \exp\left(-\frac{|\mathbf{v}|^2}{\sqrt{2}}\right), & \text{if } v_1 > 0, \\ \frac{\sqrt[4]{2}(2 - \sqrt{2})}{4\pi^{3/2}} \exp\left(-\frac{|\mathbf{v}|^2}{2\sqrt{2}}\right), & \text{if } v_1 < 0. \end{cases}$$

We refer the readers to [8] for the graphical profile of this initial value. As a spectral method, the truncated expansion (3.23) is difficult to capture an accurate profile of a discontinuous function. Therefore, we focus only on the evolution of the moments. The left column of Figure 11 shows the numerical results for  $\eta = 10$  with different choices of  $M_0$  and  $M$ . All the numerical tests show that the magnitude of the stress components  $\sigma_{11}$  and  $\sigma_{22}$ , which are initially zero, increases to a certain number before decreasing again. Such phenomenon cannot be captured by the simple BGK-type models. The lines corresponding to the results of  $M_0 = 10$ ,  $M = 40$  and  $M_0 = 15$ ,  $M = 60$  are very close to each other, which indicates that they might be very close to the exact solution. For the case  $M_0 = 5$ ,  $M = 20$ , although an obvious error can be observed, the trends of the evolution are qualitatively correct, and thus the corresponding collision model  $\mathcal{Q}_5[f]$  may also be used as a better alternative to the BGK-type models. For the heat flux  $q_1$ , the three results are hardly distinguishable.

The right column of Figure 11 gives the same moments for the soft potential  $\eta = 3.1$ . For comparison purpose, the horizontal axes are the scaled time  $t_s = t/\tau$ , where

$$\tau = \frac{4^{\frac{2}{\eta-1}-\frac{2}{9}} \tilde{B}_2^{10} \Gamma(34/9)}{\tilde{B}_2^\eta \Gamma(4 - 2/(\eta - 1))} \approx 2.03942. \quad (4.2)$$

By such scaling, the two models  $\eta = 10$  and  $\eta = 3.1$  have the same mean relaxation time near equilibrium. The two columns in Figure 11 show quite different behavior for different collision models, while both numerical results indicate the high efficiency of this method in capturing the behavior of the moments.

## 5 Concluding remarks and comparison with similar works

This work aims at an affordable way to model and simulate the binary collision between gas molecules. Our new attempt is an intermediate approach between a direct discretization of the quadratic Boltzmann collision operator and simple modelling methods like BGK-type operators. In detail, we first focus on the relatively important physical quantities, which are essentially the first few coefficients in the Hermite expansion, and use an intricate and accurate way to describe their evolution. The strategy comes from the discretization of the quadratic collision operator. For the less important quantities, we borrow the idea of the BGK-type operators and let them converge to the equilibrium at a constant rate. Although the first part is computationally expensive, we can restrict the number of degrees of freedom such that the computational cost is acceptable. The accuracy of such a model depends apparently on the size of the accurately modelled part.

In the literature, there are already some works implementing the Hermite spectral method using different algorithms, among which [17, 30] is essentially the same as ours. The difference is the implementation: the work [17] uses orthogonal polynomials based on spherical coordinates in the three-dimensional Euclidean space, while we use the orthogonal polynomials based on the

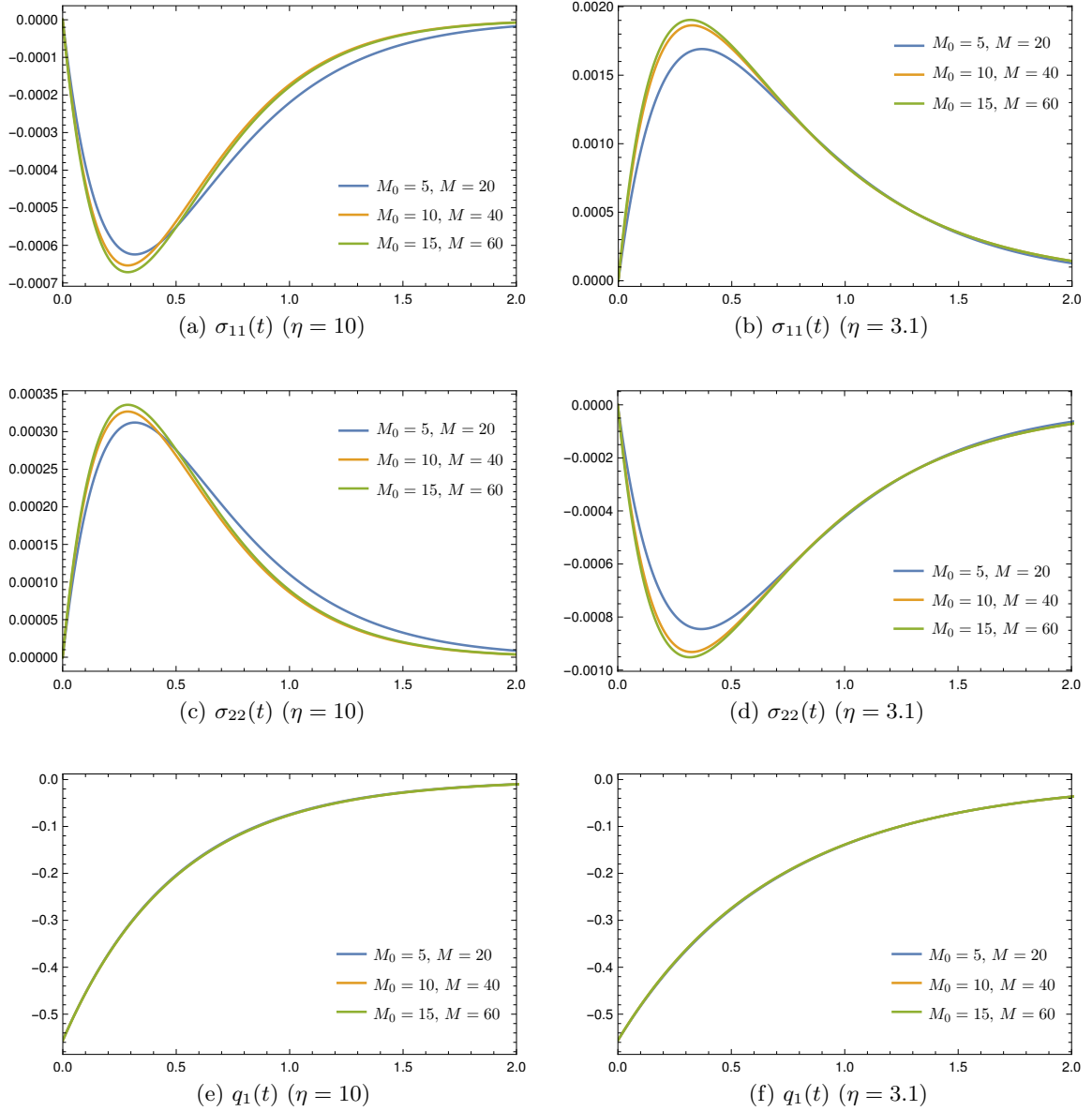


Figure 11: Evolution of the stress and the heat flux. The left column shows the results for  $\eta = 10$ , and the right column shows the results for  $\eta = 3.1$ . In the right column, the horizontal axes are the scaled time (see (4.2) and the context for details).

Cartesian coordinates; the work [30] uses the same orthogonal polynomials as ours, while the proposed computational cost in [30] is  $O(M^7)$ . Compared with [17], in which the coefficients are computed numerically, we can compute all the coefficients  $A_{k_1 k_2 k_3}^{i_1 i_2 i_3, j_1 j_2 j_3}$  almost exactly, except for the one-dimensional integration in (3.15). Compared with the algorithm in [30], our method has a higher time complexity  $O(M^9)$  if the full quadratic collision operator is used. Despite this, one can directly compare the computational time for both algorithms. It seems that our algorithm is still faster when  $M$  is small, due to a larger constant hidden in front of their computational cost  $M^7$ . One obvious deficiency of our algorithm is the memory cost as listed in Table 2. We need  $O(M^9)$  while [30] needs only  $O(M^4)$ . The reason of such a difference is that the work [30]



has shifted most of our calculation in the appendix to the online computation, whereas we store these intermediate results in memory. This leads to different memory cost for the two algorithms. Moving these computations online also makes it possible to reduce the time complexity. Thus our algorithm to compute the full quadrature collision operator will eventually be slower as  $M$  increases. Therefore in Section 3.3.2, we proposed a remedy to allow computations with a large  $M$ .

Another related work is [22], where the basis functions are chosen such that the discretization is in the  $L^2$  space instead of the weighted  $L^2$  space. One advantage of this method is that  $L^2(\mathbb{R}^3)$  is a large space, and more distribution functions can be included to the framework. However, since the coefficients in the expansion are not directly related to the moments, and the trick of cost reduction in Section 3.3.2 is not applicable.

Our numerical examples show that our method can efficiently capture the evolution of lower-order moments in the spatially homogeneous Boltzmann equation. The method should be further validated in the numerical tests for the full Boltzmann equation with spatial variables, by which one can probably get a proper *a priori* estimation of  $M_0$ . Some preliminary applications to several benchmark problems have been done in [24], and more experiments are to be carried out in future works. Besides, we are also working on a better choice of the ‘‘BGK part’’ in our collision model and the reduction of the computational cost for the quadratic part.

## Acknowledgements

We would like to thank Prof. Manuel Torrilhon at RWTH Aachen University, Germany for motivating this research project and Prof. Ruo Li at Peking University, China for the valuable suggestions to this research project. Zhenning Cai is supported by National University of Singapore Startup Fund under Grant No. R-146-000-241-133. Yanli Wang is supported by the National Natural Scientific Foundation of China (Grant No. 11501042 and 91630310).

## A Proof of Theorem 1

In order to prove Theorem 1, we first introduce the lemma below:

**Lemma 3.** *Let  $\mathbf{v} = \mathbf{h} + \mathbf{g}/2$  and  $\mathbf{w} = \mathbf{h} - \mathbf{g}/2$ . It holds that*

$$H^{k_1 k_2 k_3}(\mathbf{v}) H^{l_1 l_2 l_3}(\mathbf{w}) = \sum_{k'_1 + l'_1 = k_1 + l_1} \sum_{k'_2 + l'_2 = k_2 + l_2} \sum_{k'_3 + l'_3 = k_3 + l_3} a_{k'_1 l'_1}^{k_1 l_1} a_{k'_2 l'_2}^{k_2 l_2} a_{k'_3 l'_3}^{k_3 l_3} H^{k'_1 k'_2 k'_3}(\sqrt{2}\mathbf{h}) H^{l'_1 l'_2 l'_3} \left( \frac{\mathbf{g}}{\sqrt{2}} \right),$$

where the coefficients  $a_{k'_s l'_s}^{k_s l_s}$ ,  $s = 1, 2, 3$  are defined in (3.7).

*Proof of Lemma 3.* First, it is easy to verify that  $\exp\left(-\frac{|\mathbf{v}|^2 + |\mathbf{w}|^2}{2}\right) = \exp\left(-\left(|\mathbf{h}|^2 + \frac{|\mathbf{g}|^2}{4}\right)\right)$  and  $d\mathbf{v} d\mathbf{w} = d\mathbf{g} d\mathbf{h}$ . Based on the orthogonality of the Hermite polynomials (2.18), we just need to prove

$$\zeta_{k'_1 k'_2 k'_3, l'_1 l'_2 l'_3}^{k_1 k_2 k_3, l_1 l_2 l_3} = \begin{cases} k'_1! k'_2! k'_3! l'_1! l'_2! l'_3! a_{k'_1 l'_1}^{k_1 l_1} a_{k'_2 l'_2}^{k_2 l_2} a_{k'_3 l'_3}^{k_3 l_3}, & \text{if } k_s + l_s = k'_s + l'_s, \quad \forall s = 1, 2, 3, \\ 0, & \text{otherwise,} \end{cases} \quad (\text{A.1})$$

where the left hand side is defined as

$$\zeta_{k_1'k_2'k_3',l_1'l_2'l_3}^{k_1k_2k_3,l_1l_2l_3} := \int_{\mathbb{R}^3} \int_{\mathbb{R}^3} H^{k_1k_2k_3}(\mathbf{v}) H^{l_1l_2l_3}(\mathbf{w}) H^{k_1'k_2'k_3'}(\sqrt{2}\mathbf{h}) H^{l_1'l_2'l_3'}\left(\frac{\mathbf{g}}{\sqrt{2}}\right) \exp\left(-\frac{|\mathbf{v}|^2 + |\mathbf{w}|^2}{2}\right) d\mathbf{v} d\mathbf{w}. \quad (\text{A.2})$$

By the general Leibniz rule, we have the following relation for the derivatives of with respect to  $\mathbf{v}$ ,  $\mathbf{w}$  and  $\mathbf{g}$ ,  $\mathbf{h}$ :

$$\frac{\partial^{k_s+l_s}}{\partial v_s^{k_s} \partial w_s^{l_s}} = \sum_{i_s=0}^{k_s} \sum_{j_s=0}^{l_s} \binom{k_s}{i_s} \binom{l_s}{j_s} \frac{(-1)^{l_s-j_s}}{2^{i_s+j_s}} \frac{\partial^{k_s}}{\partial h_s^{i_s+j_s}} \frac{\partial^{l_s}}{\partial g_s^{i_s'+j_s'}}, \quad i_s' = k_s - i_s, \quad j_s' = l_s - j_s, \quad s = 1, 2, 3. \quad (\text{A.3})$$

Then, following the definition of Hermite polynomials (2.17) and (A.3), and using integration by parts, we arrive at

$$\zeta_{k_1'k_2'k_3',l_1'l_2'l_3}^{k_1k_2k_3,l_1l_2l_3} = \int_{\mathbb{R}^3} \int_{\mathbb{R}^3} \exp\left(-\left(|\mathbf{h}|^2 + \frac{|\mathbf{g}|^2}{4}\right)\right) \times \prod_{s=1}^3 \left( \sum_{i_s=0}^{k_s} \sum_{j_s=0}^{l_s} \binom{k_s}{i_s} \binom{l_s}{j_s} \frac{(-1)^{l_s-j_s}}{2^{i_s+j_s}} \frac{\partial^{k_s+l_s}}{\partial h_s^{i_s+j_s} \partial g_s^{i_s'+j_s'}} \right) H^{k_1'k_2'k_3'}(\sqrt{2}\mathbf{h}) H^{l_1'l_2'l_3'}\left(\frac{\mathbf{g}}{\sqrt{2}}\right) d\mathbf{h} d\mathbf{g}. \quad (\text{A.4})$$

From the orthogonality of Hermite polynomials and the differentiation relation

$$\frac{\partial}{\partial v_s} H^{k_1k_2k_3}(\mathbf{v}) = \begin{cases} 0, & \text{if } k_s = 0, \\ k_s H^{k_1-\delta_{1s},k_2-\delta_{2s},k_3-\delta_{3s}}(\mathbf{v}), & \text{if } k_s > 0, \end{cases} \quad (\text{A.5})$$

it holds that (A.4) is nonzero only when  $i_s + j_s = k_s'$ ,  $i_s' + j_s' = l_s'$ ,  $s = 1, 2, 3$ , which means

$$k_s + l_s = k_s' + l_s', \quad \forall s = 1, 2, 3. \quad (\text{A.6})$$

When (A.6) holds, we can apply (A.5) to (A.4) and get

$$\frac{\zeta_{k_1'k_2'k_3',l_1'l_2'l_3}^{k_1k_2k_3,l_1l_2l_3}}{k_1'!k_2'!k_3'!l_1'!l_2'!l_3'!} = \prod_{s=1}^3 \left( \sum_{i_s=0}^{k_s} \sum_{j_s=0, i_s+j_s=k_s'}^{l_s} \binom{k_s}{i_s} \binom{l_s}{j_s} \frac{(-1)^{l_s-k_s+i_s}}{2^{k_s'}} 2^{\frac{k_s'-l_s'}{2}} \right) = a_{k_1'l_1}^{k_1l_1} a_{k_2'l_2}^{k_2l_2} a_{k_3'l_3}^{k_3l_3}. \quad (\text{A.7})$$

Thus (A.1) is shown, which completes the proof of the lemma.  $\square$

**Corollary 1.** *Let  $\mathbf{v} = \mathbf{h} + \mathbf{g}/2$ . We have*

$$H^{k_1k_2k_3}(\mathbf{v}) = \sum_{l_1+m_1=k_1} \sum_{l_2+m_2=k_2} \sum_{l_3+m_3=k_3} \frac{2^{-k/2} k_1! k_2! k_3!}{l_1! l_2! l_3! m_1! m_2! m_3!} H^{l_1l_2l_3}(\sqrt{2}\mathbf{h}) H^{m_1m_2m_3}\left(\frac{\mathbf{g}}{\sqrt{2}}\right).$$

*Proof of Corollary 1.* This corollary is just a special case of Lemma 3 when  $l_1 = l_2 = l_3 = 0$ .  $\square$

*Proof of Theorem 1.* Let  $\mathbf{w} = \mathbf{v}'$ ,  $\mathbf{w}_1 = \mathbf{v}'_1$ ,  $\mathbf{s} = \mathbf{w} - \mathbf{w}_1$  and define the unit vector  $\tilde{\mathbf{n}}$  as  $\tilde{\mathbf{n}} = -(\mathbf{g} \sin \chi / |\mathbf{g}| + \mathbf{n} \cos \chi)$ . It holds that

$$\begin{aligned} |\mathbf{v}|^2 + |\mathbf{v}_1|^2 &= |\mathbf{w}|^2 + |\mathbf{w}_1|^2, & d\mathbf{v} d\mathbf{v}_1 &= d\mathbf{w} d\mathbf{w}_1, & |\mathbf{s}| &= |\mathbf{g}|, & \mathbf{s} \cdot \mathbf{n}_w &= 0, \\ \mathbf{w}' &= \cos^2(\chi/2)\mathbf{w} + \sin^2(\chi/2)\mathbf{w}_1 - |\mathbf{s}| \cos(\chi/2) \sin(\chi/2)\mathbf{n}_w = \mathbf{v}, \end{aligned} \quad (\text{A.8})$$

Following (A.8), and by change of variables, we arrive at

$$\begin{aligned}
& \int_{\mathbb{R}^3} \int_{\mathbb{R}^3} \int_{\mathbf{n} \perp \mathbf{g}} \int_0^\pi B(|\mathbf{g}|, \chi) H^{i_1 i_2 i_3}(\mathbf{v}') H^{j_1 j_2 j_3}(\mathbf{v}'_1) H^{k_1 k_2 k_3}(\mathbf{v}) \exp\left(-\frac{|\mathbf{v}|^2 + |\mathbf{v}_1|^2}{2}\right) d\chi d\mathbf{n} d\mathbf{v}_1 d\mathbf{v} \\
&= \int_{\mathbb{R}^3} \int_{\mathbb{R}^3} \int_{\tilde{\mathbf{n}} \perp \mathbf{s}} \int_0^\pi B(|\mathbf{s}|, \chi) H^{i_1 i_2 i_3}(\mathbf{w}) H^{j_1 j_2 j_3}(\mathbf{w}_1) H^{k_1 k_2 k_3}(\mathbf{w}') \exp\left(-\frac{|\mathbf{w}|^2 + |\mathbf{w}_1|^2}{2}\right) d\chi d\tilde{\mathbf{n}} d\mathbf{w}_1 d\mathbf{w} \\
&= \int_{\mathbb{R}^3} \int_{\mathbb{R}^3} \int_{\mathbf{n} \perp \mathbf{g}} \int_0^\pi B(|\mathbf{g}|, \chi) H^{i_1 i_2 i_3}(\mathbf{v}) H^{j_1 j_2 j_3}(\mathbf{v}_1) H^{k_1 k_2 k_3}(\mathbf{v}') \exp\left(-\frac{|\mathbf{v}|^2 + |\mathbf{v}_1|^2}{2}\right) d\chi d\mathbf{n} d\mathbf{v}_1 d\mathbf{v}.
\end{aligned} \tag{A.9}$$

Thus, we can substitute the above equality into (3.4) to get

$$\begin{aligned}
A_{k_1 k_2 k_3}^{i_1 i_2 i_3, j_1 j_2 j_3} &= \frac{1}{(2\pi)^3 k_1! k_2! k_3!} \int_{\mathbb{R}^3} \int_{\mathbb{R}^3} \int_{\mathbf{n} \perp \mathbf{g}} \int_0^\pi B(|\mathbf{g}|, \chi) [H^{k_1 k_2 k_3}(\mathbf{v}') - H^{k_1 k_2 k_3}(\mathbf{v})] \\
&\quad H^{i_1 i_2 i_3}(\mathbf{v}) H^{j_1 j_2 j_3}(\mathbf{v}_1) \exp\left(-\frac{|\mathbf{v}|^2 + |\mathbf{v}_1|^2}{2}\right) d\chi d\mathbf{n} d\mathbf{v}_1 d\mathbf{v}.
\end{aligned} \tag{A.10}$$

Further simplification of (A.10) follows the method in [21], where the velocity of the mass center is defined as  $\mathbf{h} = (\mathbf{v} + \mathbf{v}_1)/2 = (\mathbf{v}' + \mathbf{v}'_1)/2$ . Hence,

$$\mathbf{v} = \mathbf{h} + \frac{1}{2}\mathbf{g}, \quad \mathbf{v}_1 = \mathbf{h} - \frac{1}{2}\mathbf{g}, \quad \mathbf{v}' = \mathbf{h} + \frac{1}{2}\mathbf{g}', \quad \mathbf{v}'_1 = \mathbf{h} - \frac{1}{2}\mathbf{g}', \tag{A.11}$$

$$|\mathbf{v}|^2 + |\mathbf{v}_1|^2 = \frac{1}{2}|\mathbf{g}|^2 + 2|\mathbf{h}|^2, \quad d\mathbf{v} d\mathbf{v}_1 = d\mathbf{g} d\mathbf{h}. \tag{A.12}$$

Combining Lemma 3, Corollary 1 and (A.12), we can rewrite (A.10) as an integral with respect to  $\mathbf{g}$  and  $\mathbf{h}$ :

$$\begin{aligned}
A_{k_1 k_2 k_3}^{i_1 i_2 i_3, j_1 j_2 j_3} &= \sum_{i'_1 + j'_1 = i_1 + j_1} \sum_{i'_2 + j'_2 = i_2 + j_2} \sum_{i'_3 + j'_3 = i_3 + j_3} \sum_{l'_1 + k'_1 = k_1} \sum_{l'_2 + k'_2 = k_2} \sum_{l'_3 + k'_3 = k_3} \\
&\quad \frac{2^{-k/2}}{(2\pi)^3} \frac{1}{k'_1 k'_2 k'_3 l'_1! l'_2! l'_3!} a_{i'_1 j'_1}^{i_1 j_1} a_{i'_2 j'_2}^{i_2 j_2} a_{i'_3 j'_3}^{i_3 j_3} \gamma_{j'_1 j'_2 j'_3}^{l'_1 l'_2 l'_3} \eta_{i'_1 i'_2 i'_3}^{k'_1 k'_2 k'_3},
\end{aligned} \tag{A.13}$$

where the coefficients  $\gamma_{j'_1 j'_2 j'_3}^{l'_1 l'_2 l'_3}$  defined in (3.8) are integrals with respect to  $\mathbf{g}$ , and  $\eta_{i'_1 i'_2 i'_3}^{k'_1 k'_2 k'_3}$  are integrals with respect to  $\mathbf{h}$  defined by

$$\eta_{i'_1 i'_2 i'_3}^{k'_1 k'_2 k'_3} = \int_{\mathbb{R}^3} H^{i'_1 i'_2 i'_3}(\sqrt{2}\mathbf{h}) H^{k'_1 k'_2 k'_3}(\sqrt{2}\mathbf{h}) \exp(-|\mathbf{h}|^2) d\mathbf{h} = \pi^{3/2} k'_1! k'_2! k'_3! \delta_{i'_1 k'_1} \delta_{i'_2 k'_2} \delta_{i'_3 k'_3}. \tag{A.14}$$

Thus the theorem is proven by substituting (A.14) into (A.13).  $\square$

## B Proof of Theorem 2

We will first prove Theorem 2 based on several lemmas, and then prove these lemmas.

### B.1 Proof of Theorem 2

In order to prove Theorem 2, we will introduce the definition of Ikenberry polynomials [26] and several lemmas.

**Definition 4** (Ikenberry polynomials). Let  $\mathbf{v} = (v_1, v_2, v_3)^T \in \mathbb{R}^3$ . For  $\forall n \in \mathbb{N}$ , and  $i_1, \dots, i_n \in \{1, 2, 3\}$ , define  $Y_{i_1 \dots i_n}(\mathbf{v})$  as the Ikenberry polynomials

$$Y(\mathbf{v}) = 1, \quad Y_{i_1}(\mathbf{v}) = v_{i_1},$$

$$Y_{i_1 \dots i_n}(\mathbf{v}) = v_{i_1} \cdots v_{i_n} + |\mathbf{v}|^2 S_{n-2}^{i_1 \dots i_n}(\mathbf{v}) + |\mathbf{v}|^4 S_{n-4}^{i_1 \dots i_n} + \cdots + |\mathbf{v}|^{2\lfloor n/2 \rfloor} S_{n-2\lfloor n/2 \rfloor}^{i_1 \dots i_n}(\mathbf{v}),$$

where  $S_j^{i_1 \dots i_n}$  is a homogeneous harmonic polynomial of degree  $j$  defined in [26], which can be determined by

$$\Delta_{\mathbf{v}} Y_{i_1 \dots i_n} = \Delta_{\mathbf{v}}^2 Y_{i_1 \dots i_n} = \Delta_{\mathbf{v}}^{\lfloor n/2 \rfloor} Y_{i_1 \dots i_n} = 0.$$

For  $k_1, k_2, k_3 \in \mathbb{N}$ , define  $Y^{k_1 k_2 k_3}(\mathbf{v})$  as the polynomial  $Y_{i_1 \dots i_n}(\mathbf{v})$  with

$$n = k_1 + k_2 + k_3, \quad i_1 = \cdots = i_{k_1} = 1,$$

$$i_{k_1+1} = \cdots = i_{k_1+k_2} = 2, \quad i_{k_1+k_2+1} = \cdots = i_n = 3.$$

**Lemma 4.** The integral

$$\int_{\mathbb{S}^2} Y^{k_1 k_2 k_3}(\mathbf{n}) Y^{l_1 l_2 l_3}(\mathbf{n}) d\mathbf{n}$$

is the coefficient of  $v_1^{k_1} v_2^{k_2} v_3^{k_3} w_1^{l_1} w_2^{l_2} w_3^{l_3}$  in the polynomial

$$\frac{4\pi}{2k+1} \frac{k_1! k_2! k_3! l_1! l_2! l_3!}{[(2k-1)!!]^2} (|\mathbf{v}| |\mathbf{w}|)^k P_k \left( \frac{\mathbf{v}}{|\mathbf{v}|} \cdot \frac{\mathbf{w}}{|\mathbf{w}|} \right), \quad k = k_1 + k_2 + k_3.$$

**Lemma 5.** The Hermite polynomial  $H^{k_1 k_2 k_3}(\mathbf{v})$  can be represented as

$$H^{k_1 k_2 k_3}(\mathbf{v}) = \sum_{m_1=0}^{\lfloor k_1/2 \rfloor} \sum_{m_2=0}^{\lfloor k_2/2 \rfloor} \sum_{m_3=0}^{\lfloor k_3/2 \rfloor} \frac{(-1)^m m! (2k-4m+1)!!}{(2(k-m)+1)!!} \left( \prod_{i=1}^3 \frac{k_i!}{m_i! (k_i - 2m_i)!} \right)$$

$$L_m^{(k-2m+1/2)} \left( \frac{|\mathbf{v}|^2}{2} \right) Y^{k_1-2m_1, k_2-2m_2, k_3-2m_3}(\mathbf{v}),$$

where  $k = k_1 + k_2 + k_3$  and  $m = m_1 + m_2 + m_3$ .

**Lemma 6.** Given a vector  $\mathbf{g}$  and  $\chi \in [0, \pi]$ , let  $\mathbf{g}'(\mathbf{n}) = \mathbf{g} \cos \chi - |\mathbf{g}| \mathbf{n} \sin \chi$ , where  $\mathbf{n}$  is a unit vector. It holds that

$$\int_{\mathbf{n} \perp \mathbf{g}} Y^{k_1 k_2 k_3}(\mathbf{g}'/|\mathbf{g}|) d\mathbf{n} = 2\pi Y^{k_1 k_2 k_3}(\mathbf{g}/|\mathbf{g}|) P_k(\cos \chi),$$

where  $k = k_1 + k_2 + k_3$  and  $P_k$  is Legendre polynomial.

In above lemmas, Lemma 4 and Lemma 5 will be proved in Appendix B.2 and B.3 respectively. Lemma 6 is proved in [29]. By Lemma 5 and Lemma 6, we can derive the corollary below

**Corollary 2.** Given a vector  $\mathbf{g}$  and  $\chi \in [0, \pi]$ , define  $\mathbf{g}'(\mathbf{n})$  the same as in Theorem 6. We have

$$\int_{\mathbf{n} \perp \mathbf{g}} H^{k_1 k_2 k_3}(\mathbf{g}') d\mathbf{n} = 2\pi \sum_{m_1=0}^{\lfloor k_1/2 \rfloor} \sum_{m_2=0}^{\lfloor k_2/2 \rfloor} \sum_{m_3=0}^{\lfloor k_3/2 \rfloor} \frac{(-1)^m m! (2k-4m+1)!!}{(2(k-m)+1)!!} \times$$

$$\left( \prod_{i=1}^3 \frac{k_i!}{m_i! (k_i - 2m_i)!} \right) L_n^{(k-2m+1/2)} \left( \frac{|\mathbf{g}|^2}{2} \right) Y^{k_1-2m_1, k_2-2m_2, k_3-2m_3}(\mathbf{g}) P_{k-2m}(\cos \chi),$$

where  $k = k_1 + k_2 + k_3$ ,  $m = m_1 + m_2 + m_3$ .

*Proof of Theorem 2.* By Lemma 5, the corollary 2 and the homogeneity of the Ikenberry polynomials  $\gamma_{k_1 k_2 k_3}^{l_1 l_2 l_3}$  defined in (3.9) can be simplified as

$$\begin{aligned} \gamma_{k_1 k_2 k_3}^{l_1 l_2 l_3} &= 2\pi \sum_{m_1=0}^{\lfloor k_1/2 \rfloor} \sum_{m_2=0}^{\lfloor k_2/2 \rfloor} \sum_{m_3=0}^{\lfloor k_3/2 \rfloor} \sum_{n_1=0}^{\lfloor l_1/2 \rfloor} \sum_{n_2=0}^{\lfloor l_2/2 \rfloor} \sum_{n_3=0}^{\lfloor l_3/2 \rfloor} \frac{(2(k-m)+1)!! C_{m_1 m_2 m_3}^{k_1 k_2 k_3} (2(l-n)+1)!! C_{n_1 n_2 n_3}^{l_1 l_2 l_3}}{4\pi \prod_{i=1}^3 (k_i - 2m_i)! 4\pi \prod_{i=1}^3 (l_i - 2n_i)!} \times \\ &2 \int_0^{+\infty} \int_0^\pi \int_{\mathbb{S}^2} Y^{k_1-2m_1, k_2-2m_2, k_3-2m_3}(\mathbf{n}) Y^{l_1-2n_1, l_2-2n_2, l_3-2n_3}(\mathbf{n}) \left(\frac{g}{\sqrt{2}}\right)^{k+l+2-2(m+n)} \times \\ &L_m^{(k-2m+1/2)} \left(\frac{g^2}{4}\right) L_n^{(l-2n+1/2)} \left(\frac{g^2}{4}\right) B(g, \chi) \left[ P_{k-2m}(\cos \chi) - 1 \right] \exp\left(-\frac{g^2}{4}\right) d\mathbf{n} d\chi dg, \end{aligned} \quad (\text{B.1})$$

where  $C_{m_1 m_2 m_3}^{l_1 l_2 l_3}$  is defined in (3.10).

Substituting Lemma 4 into (B.1), we complete this proof.  $\square$

## B.2 Proof of Lemma 4

In order to prove Lemma 4, we first introduce the following definitions and lemmas.

**Definition 5** (Associated Legendre functions). *For  $m = -l, \dots, l$ , the associated Legendre functions are defined as*

$$P_l^m(x) = \frac{(-1)^m}{2^l l!} (1-x^2)^{m/2} \frac{d^{l+m}}{dx^{l+m}} (x^2-1)^l.$$

**Definition 6** (Spherical harmonics). *For  $l \in \mathbb{N}$  and  $m = -l, \dots, l$ , the spherical harmonic  $Y_l^m(\theta, \varphi)$  is defined as*

$$Y_l^m(\mathbf{n}) = Y_l^m(\theta, \varphi) = \sqrt{\frac{2l+1}{4\pi} \frac{(l-m)!}{(l+m)!}} P_l^m(\cos \theta) \exp(im\varphi), \quad \mathbf{n} \in \mathbb{S}^2,$$

where  $(\theta, \varphi)$  is the spherical coordinates of  $\mathbf{n}$ .

**Lemma 7** (Addition theorem). *For any  $l \in \mathbb{N}$ , it holds that*

$$P_l(\mathbf{n}_1 \cdot \mathbf{n}_2) = \frac{4\pi}{2l+1} \sum_{m=-l}^l Y_l^m(\mathbf{n}_1) \overline{Y_l^m(\mathbf{n}_2)},$$

where  $P_l$  is Legendre polynomial.

**Lemma 8.** *For any  $l \in \mathbb{N}$ , it holds that*

$$(|\mathbf{v}||\mathbf{w}|)^l P_l\left(\frac{\mathbf{v}}{|\mathbf{v}|} \cdot \frac{\mathbf{w}}{|\mathbf{w}|}\right) = \frac{(2l)!}{2^l l! l!} \sum_{i_1=1}^3 \cdots \sum_{i_l=1}^3 w_{i_1} \cdots w_{i_l} Y_{i_1 \cdots i_l}(\mathbf{v}).$$

In the above lemmas, Lemma 7 and Lemma 8 are well-known and their proofs can be found in [1] and [27] respectively. Based on these two lemmas, the following corollary holds.

**Corollary 3.** *The harmonic polynomial  $Y^{k_1 k_2 k_3}(\mathbf{v})$  is the coefficient of the monomial  $w_1^{k_1} w_2^{k_2} w_3^{k_3}$  in the following polynomial of  $\mathbf{w}$ :*

$$\frac{k_1! k_2! k_3!}{(2k-1)!!} (|\mathbf{v}||\mathbf{w}|)^k P_k\left(\frac{\mathbf{v}}{|\mathbf{v}|} \cdot \frac{\mathbf{w}}{|\mathbf{w}|}\right), \quad k = k_1 + k_2 + k_3.$$

*Proof of Corollary 3.* Since

$$\sum_{i_1=1}^3 \cdots \sum_{i_k=1}^3 w_{i_1} \cdots w_{i_k} Y_{i_1 \cdots i_k}(\mathbf{v}) = \frac{k!}{k_1!k_2!k_3!} \sum_{k_1+k_2+k_3=k} w_1^{k_1} w_2^{k_2} w_3^{k_3} Y^{k_1 k_2 k_3}(\mathbf{v}),$$

and matching the term of  $w_1^{k_1} w_2^{k_2} w_3^{k_3}$  in Lemma 8, we complete this proof.  $\square$

*Proof of Lemma 4.* From Corollary 3, we can derive that  $\int_{\mathbb{S}^2} Y^{k_1 k_2 k_3}(\mathbf{n}) Y^{l_1 l_2 l_3}(\mathbf{n}) d\mathbf{n}$  is the coefficient of  $v_1^{k_1} v_2^{k_2} v_3^{k_3} w_1^{l_1} w_2^{l_2} w_3^{l_3}$  in the polynomial

$$\int_{\mathbb{S}^2} \left[ \beta^{k_1 k_2 k_3} (|\mathbf{n}| |\mathbf{v}|)^k P_k \left( \mathbf{n} \cdot \frac{\mathbf{v}}{|\mathbf{v}|} \right) \right] \left[ \beta^{l_1 l_2 l_3} (|\mathbf{n}| |\mathbf{w}|)^l P_l \left( \mathbf{n} \cdot \frac{\mathbf{w}}{|\mathbf{w}|} \right) \right] d\mathbf{n},$$

where  $k = k_1 + k_2 + k_3, l = l_1 + l_2 + l_3$  and  $\beta^{k_1 k_2 k_3} = \frac{k_1! k_2! k_3!}{(2k-1)!!}$ . Following Theorem 7, it holds

$$\begin{aligned} & \int_{\mathbb{S}^2} \left[ (|\mathbf{n}| |\mathbf{v}|)^k P_k \left( \mathbf{n} \cdot \frac{\mathbf{v}}{|\mathbf{v}|} \right) \right] \left[ (|\mathbf{n}| |\mathbf{w}|)^l P_l \left( \mathbf{n} \cdot \frac{\mathbf{w}}{|\mathbf{w}|} \right) \right] d\mathbf{n} \\ &= (|\mathbf{v}|^k |\mathbf{w}|^l) \frac{(4\pi)^2}{(2k+1)(2l+1)} \sum_{m=-k}^k \sum_{n=-l}^l Y_k^m(\mathbf{v}) \overline{Y_l^n(\mathbf{w})} \delta_{lk} \delta_{mn} \\ &= \frac{4\pi \delta_{kl}}{2k+1} (|\mathbf{v}| |\mathbf{w}|)^k P_k \left( \frac{\mathbf{v}}{|\mathbf{v}|} \cdot \frac{\mathbf{w}}{|\mathbf{w}|} \right). \end{aligned}$$

Thus if  $k = l$ , this corollary is proved. If  $k \neq l$ , we can deduce that  $\int_{\mathbb{S}^2} Y^{k_1 k_2 k_3}(\mathbf{n}) Y^{l_1 l_2 l_3}(\mathbf{n}) d\mathbf{n} = 0$ . In this case, the coefficient of  $v_1^{k_1} v_2^{k_2} v_3^{k_3} w_1^{l_1} w_2^{l_2} w_3^{l_3}$  in the polynomial  $(|\mathbf{v}| |\mathbf{w}|)^k P_k \left( \frac{\mathbf{v}}{|\mathbf{v}|} \cdot \frac{\mathbf{w}}{|\mathbf{w}|} \right)$  is also zero, and this completes the proof.  $\square$

### B.3 Proof of Lemma 5

We will prove Lemma 5 in this section.

*Proof of Lemma 5.* Define the homogeneous spherical harmonic  $Z_{i_1 i_2 \cdots i_k}^{(k,m)}$  of degree  $k - 2m$  as

$$Z_{i_1 i_2 \cdots i_k}^{(k,m)} = \frac{1}{k!} \sum_{\sigma \in \mathcal{S}_k} Y_{i_{\sigma(1)} i_{\sigma(2)} \cdots i_{\sigma(r)}} \delta_{i_{\sigma(r+1)} i_{\sigma(r+2)}} \cdots \delta_{i_{\sigma(k-1)} i_{\sigma(k)}}, \quad (\text{B.2})$$

where  $r = k - 2m$  and the sum is taken over all permutations of the set  $\{1, 2, \dots, k\}$ , i.e.

$$\mathcal{S}_k = \{\sigma \mid \sigma : \{1, 2, \dots, k\} \rightarrow \{1, 2, \dots, k\} \text{ is a bijection}\}.$$

It has been proven in [28, eqs. (3)(8)(9)(31)] that <sup>1</sup>

$$H^{k_1 k_2 k_3}(\mathbf{v}) = \sum_{m=0}^{\lfloor k/2 \rfloor} \frac{(-1)^m k! (2k - 4m + 1)!!}{(k - 2m)! (2k - 2m + 1)!!} L_m^{(k-2m+1/2)} \left( \frac{|\mathbf{v}|^2}{2} \right) Z_{i_1 i_2 \cdots i_k}^{(k,m)}(\mathbf{v}), \quad (\text{B.3})$$

where the indices  $i_1, \dots, i_k$  satisfy:

$$i_1 = \cdots = i_{k_1} = 1, \quad i_{k_1+1} = \cdots = i_{k_1+k_2} = 2, \quad i_{k_1+k_2+1} = \cdots = i_k = 3.$$

<sup>1</sup>In [28], the definition of the Laguerre polynomial differs from Definition 3 by a constant, which makes the coefficient in our paper slightly different from the one in [28].

To prove Lemma 5, we just need to provide a more explicit expression for (B.2). In order that the summand in (B.2) is nonzero, the two indices of every Kronecker symbol must be the same. When all the Kronecker symbols take  $2m_1$  ones,  $2m_2$  twos and  $2m_3$  threes as their indices, the summand will actually be  $Y^{k_1-2m_1, k_2-2m_2, k_3-2m_3}(\mathbf{v})$  according to Definition 4. Apparently  $(m_1, m_2, m_3)$  must be indices from the following set:

$$\mathcal{M}_{k_1 k_2 k_3}^m = \{(m_1, m_2, m_3) \mid m_1 + m_2 + m_3 = m, 2m_1 \leq k_1, 2m_2 \leq k_2, 2m_3 \leq k_3\}.$$

Next, we are going to count how many times  $Y^{k_1-2m_1, k_2-2m_2, k_3-2m_3}(\mathbf{v})$  appears in the sum in (B.2). This can be observed by noting that

1. The  $m$  Kronecker symbols choosing from  $m_1$  pairs of ones,  $m_2$  pairs of twos and  $m_3$  pairs of threes gives a factor  $m!/(m_1!m_2!m_3!)$ ;
2. The  $k - 2m$  indices of  $Y$  choosing from  $k_1 - 2m_1$  ones,  $k_2 - 2m_2$  twos and  $k_3 - 2m_3$  threes gives a factor  $(k - 2m)!/((k_1 - 2m_1)!(k_2 - 2m_2)!(k_3 - 2m_3)!)$ .
3. Permutations of  $k_1$  ones,  $k_2$  twos and  $k_3$  threes give respectively factors  $k_1!$ ,  $k_2!$  and  $k_3!$ .

Summarizing all these results, we get

$$Z_{i_1 i_2 \dots i_k}^{(k, m)} = \frac{1}{k!} \sum_{(m_1, m_2, m_3) \in \mathcal{M}_{k_1 k_2 k_3}^m} \frac{(k - 2m)! m! \prod_{i=1}^3 k_i!}{\prod_{i=1}^3 ((k_i - 2m_i)! m_i!)} Y^{k_1-2m_1, k_2-2m_2, k_3-2m_3}(\mathbf{v}). \quad (\text{B.4})$$

By (B.3) and (B.4), the proof is completed.  $\square$

## References

- [1] G. B. Arfken, H. J. Weber, and D. Spector. Mathematical Methods for Physicists, 4th ed. *Am. J. Phys.*, 67:165–169, February 1999.
- [2] P. L. Bhatnagar, E. P. Gross, and M. Krook. A model for collision processes in gases. I. small amplitude processes in charged and neutral one-component systems. *Phys. Rev.*, 94(3):511–525, 1954.
- [3] G. A. Bird. *Molecular Gas Dynamics and the Direct Simulation of Gas Flows*. Oxford: Clarendon Press, 1994.
- [4] Z. Cai, Y. Fan, and L. Ying. An entropic fourier method for the Boltzmann equation. *SIAM J. Sci. Comput.*, 40(5):A2858–A2882, 2018.
- [5] Z. Cai, R. Li, and Z. Qiao. NRxx simulation of microflows with shakhov model. *SIAM J. Sci. Comput.*, 34(1):A339–A369, 2012.
- [6] Z. Cai, R. Li, and Z. Qiao. Globally hyperbolic regularized moment method with applications to microflow simulation. *Comput. Fluids*, 81:95–109, 2013.
- [7] Z. Cai, R. Li, and Y. Wang. An efficient NRxx method for Boltzmann-BGK equation. *J. Sci. Comput.*, 50(1):103–119, 2012.

- [8] Z. Cai and M. Torrilhon. Approximation of the linearized Boltzmann collision operator for hard-sphere and inverse-power-law models. *J. Comput. Phys.*, 295:617–643, 2015.
- [9] S. Chapman and T. G. Cowling. *The Mathematical Theory of Non-uniform Gases, Third Edition*. Cambridge University Press, 1990.
- [10] S. Chen, K. Xu, and Q. Cai. A comparison and unification of ellipsoidal statistical and Shakhov BGK models. *Adv. Appl. Math. Mech.*, 7(2):245–266, 2015.
- [11] G. Dimarco, R. Loubère, and J. Narski. Towards an ultra efficient kinetic scheme. Part III: High-performance-computing. *J. Comput. Phys.*, 284:22–39, 2015.
- [12] G. Dimarco, R. Loubère, J. Narski, and T. Rey. An efficient numerical method for solving the Boltzmann equation in multidimensions. *J. Comput. Phys.*, 353:46–81, 2018.
- [13] G. Dimarco and L. Pareschi. Numerical methods for kinetic equations. *Acta Numerica*, 23:369–520, 2014.
- [14] F. Filbet, C. Mouhot, and L. Pareschi. Solving the Boltzmann equation in  $N \log_2 N$ . *SIAM J. on Sci. Comput.*, 28(3):1029–1053, 2006.
- [15] F. Filbet, L. Pareschi, and T. Rey. On steady-state preserving spectral methods for homogeneous Boltzmann equations. *Comptes Rendus Mathématique*, 353(4):309–314, 2015.
- [16] I. M. Gamba, J. R. Haack, C. D. Hauck, and J. Hu. A fast spectral method for the Boltzmann collision operator with general collision kernels. *SIAM J. Sci. Comput.*, 39(4):B658–B674, 2017.
- [17] I. M. Gamba and S. Rjasanow. Galerkin-Petrov approach for the Boltzmann equation. *J. Comput. Phys.*, 366:341–365, 2018.
- [18] I. M. Gamba and S. H. Tharkabhusanam. Spectral-Lagrangian methods for collisional models of non-equilibrium statistical states. *J. Comput. Phys.*, 228(6):2012–2036, 2009.
- [19] W. Gao and Q. Sun. Evaluation of BGK-type models of the Boltzmann equation. In J. Fan, editor, *Proceedings of the 29th International Symposium on Rarefied Gas Dynamics*, volume 1628, pages 84–91, 2014.
- [20] D. Goldstein, B. Sturtevant, and J. E. Broadwell. Investigations of the motion of discrete-velocity gases. *Progress in Astronautics and Aeronautics*, 117:100–117, 1989.
- [21] H. Grad. On the kinetic theory of rarefied gases. *Comm. Pure Appl. Math.*, 2(4):331–407, 1949.
- [22] P. Grohs, R. Hiptmair, and S. Pintarelli. Tensor-product discretization for the spatially inhomogeneous and transient Boltzmann equation in two dimensions. *SIAM J. Comput. Math.*, 3:219–248, 2017.
- [23] L. H. Holway. New statistical models for kinetic theory: Methods of construction. *Phys. Fluids*, 9(1):1658–1673, 1966.
- [24] Z. Hu, Z. Cai, and Y. Wang. Numerical simulation of microflows using Hermite spectral methods, 2018. Submitted. arXiv: 1807.06236.



- [25] J. C. Huang, K. Xu, and P. Yu. A unified gas-kinetic scheme for continuum and rarefied flows II: Multi-dimensional cases. *Commun. Comput. Phys.*, 12:662–690, 2012.
- [26] E. Ikenberry. A system of homogeneous spherical harmonics. *Am. Math. Mon.*, 62(10):719–721, 1955.
- [27] E. Ikenberry. A system of homogeneous spherical harmonics. *J. Math. Anal. Appl.*, 3:355–357, 1961.
- [28] E. Ikenberry. Representation of Grad’s Hermite polynomials as sums of products of Sonine polynomials and solid spherical harmonics. *Arch. Rat. Mech. Anal.*, 9:255–259, 1962.
- [29] E. Ikenberry and C. Truesdell. On the pressures and the flux of energy in a gas according to Maxwell’s kinetic theory I. *J. Rat. Mech. Anal.*, 5(1):1–54, 1956.
- [30] G. Kitzler and J. Schröberl. A polynomial spectral method for the spatially homogeneous Boltzmann equation. *SIAM J. Sci. Comput.*, 41(1):B27–B49, 2019.
- [31] K. Kumar. Polynomial expansions in kinetic theory of gases. *Ann. Phys.*, 37:113–141, 1966.
- [32] C. Mouhot and L. Pareschi. Fast algorithms for computing the Boltzmann collision operator. *Math. Comp.*, 75(256):1833–1852, 2006.
- [33] A. V. Panferov and A. G. Heintz. A new consistent discrete-velocity model for the Boltzmann equation. *Math. Method Appl. Sci.*, 25(7):571–593, 2002.
- [34] L. Pareschi and B. Perthame. A fourier spectral method for homogeneous Boltzmann equations. *Transport Theor. Stat.*, 25(3-5):369–382, 1996.
- [35] L. Pareschi and G. Russo. On the stability of spectral methods for the homogeneous Boltzmann equation. *Trans. Theory Stat. Phys.*, 29(3–5):431–447, 2000.
- [36] R. Piessens, E. de Doncker-Kapenga, C.W. Überhuber, and D.K. Kahaner. *Quadpack — A Subroutine Package for Automatic Integration*. Springer, 1983.
- [37] E. M. Shakhov. Generalization of the Krook kinetic relaxation equation. *Fluid Dyn.*, 3(5):95–96, 1968.
- [38] H. M. Srivastava, H. A. Mavromatis, and R. S. Alassar. Remarks on some associated Laguerre integral results. *Appl. Math. Lett.*, 16(7):1131–1136, 2003.
- [39] C. Truesdell and R. G. Muncaster. *Fundamentals of Maxwell’s Kinetic Theory of a Simple Monatomic Gas: Treated as a Branch of Rational Mechanics*. Academic Press, 1980.
- [40] L. Wu, J. M. Reese, and Y. Zhang. Solving the Boltzmann equation deterministically by the fast spectral method: application to gas microflows. *J. Fluid Mech.*, 746:53–84, 2014.